Electronic Supplementary Material (ESI) for ChemComm.
This journal is © The Royal Society of Chemistry 2020

Electronic Supporting Information

Preparation and reactivity of molybdenum complexes bearing pyrrole-based PNP-type pincer ligand

Yoshiaki Tanabe,[a] Yoshiya Sekiguchi,[a] Hiromasa Tanaka,[b] Asuka Konomi,[b] Kazunari Yoshizawa,[b] Shogo Kuriyama[a] and Yoshiaki Nishibayashi*[a]

[a] Department of Systems Innovation, School of Engineering, The University of Tokyo, Hongo, Bunkyo-ku, Tokyo 113-8656, Japan. E-mail: ynishiba@sys.t.u-tokyo.ac.jp.
[b] Institute for Materials Chemistry and Engineering, Kyushu University, Nishi-ku, Fukuoka 819-0395, Japan. E-mail: kazunari@ms.ifoc.kyushu-u.ac.jp.

Table of Contents

General methods. All manipulations were carried out under an atmosphere of dry dinitrogen or dry argon by using standard Schlenk or glovebox techniques unless otherwise stated. All solvents were dried by general methods and were degassed before use. [MoI$_3$(thf)$_3$],[S1] Li**PNP** (**PNP** = 2,5-bis(di-*tert*-butylphosphinomethyl)pyrrolide),[S2] SmI$_2$(thf)$_2$,[S3] CoCp*$_2$ (Cp* = η^5-C$_5$Me$_5$),[S4] KC$_8$,[S5] [ColH]OTf (Col = 2,4,6-trimethylpyridine, OTf = trifluoromethanesulfonate),[S6] and [H(OEt$_2$)$_2$]BAr$^F_4$ (BAr$^F_4$ = tetrakis[3,5-bis(trifluoromethyl)phenyl]borate)[S7] were prepared according to the literature. Other reagents were purchased commercially and used as received.

IR spectra were recorded on a JASCO FT/IR 4100 Fourier Transform infrared spectrometer. UV-vis absorption spectra were recorded on a Shimadzu UV-1850. Evolved dinitrogen and dihydrogen were quantified by gas chromatography using a Shimadzu GC-8A equipped with a TCD detector and a SHINCARBON ST (6 m × 3 mm). ^{1}H NMR and ^{31}P{^{1}H} NMR spectra were recorded on a JEOL ECS-400 spectrometer (^{1}H, 400 MHz; ^{31}P, 162 MHz) in suitable solvents at room temperature and were referenced to residual solvents (for ^{1}H NMR) or an external standard (85% H$_3$PO$_4$ for ^{31}P NMR). Magnetic susceptibilities were measured on a JEOL ECS-400 spectrometer by using the Evans method.[S8] Elemental analyses were performed at the Microanalytical Center of The University of Tokyo.

Preparation of [MoI$_2$(PNP)] (1). A suspension of [MoI$_3$(thf)$_3$] (138.5 mg, 0.200 mmol) and Li**PNP** (87.1 mg, 0.224 mmol) in THF (5 mL) was stirred at room temperature for 20 h under Ar (1 atm) and was dried *in vacuo* to give dark brown residue. The residue was then dissolved in toluene (5 mL × 3), and the brown suspension was filtered through a pad of Celite, where the filtrate was collected and dried *in vacuo* to give brown residue. The residue was then dissolved in diethyl ether (5 mL), concentrated *in vacuo* to *ca.* 1 mL, where hexane (5 mL) was added to give orange brown precipitate of [MoI$_2$(**PNP**)] (**1**, 118.5 mg, 0.162 mmol, 81% isolated yield) (Scheme S1). Green needle crystals of **1** suitable for X-ray analyses were obtained by slow evaporation of diethyl ether solution of **1** in Ar glovebox (Fig. S1). Magnetic susceptibility (Evans' method): $\mu_{\mathrm{eff}} = 1.4\ \mu_{\mathrm{B}}$ in C$_6$D$_6$ at 294 K. Anal. Calcd for C$_{22}$H$_{42}$I$_2$MoNP$_2$ (**1**): C, 36.08; H, 5.78; N, 1.91. Found: C, 35.86; H, 5.87; N, 1.90.

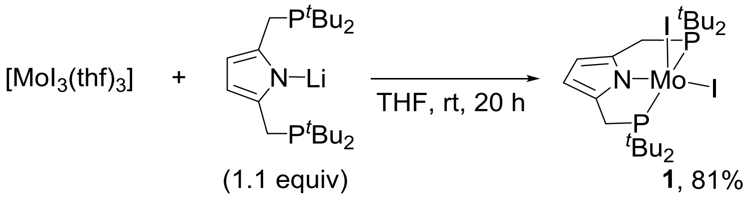

Scheme S1 Preparation of **1**.

Preliminary reduction of 1 by KC$_8$ under N$_2$ to afford [(K(N$_2$){Mo(N$_2$)(PNP)}$_2$)$_n$] (2). To a solution of **1** (73.2 mg, 0.100 mmol) in THF (5 mL) was added KC$_8$ (41.0 mg, 0.303 mmol) at –15 °C under N$_2$ (1 atm). After the solution was further stirred at –15 °C for 2 h, the mixture was warmed to room temperature, and was further stirred at room temperature for 20 h. The resultant dark purple solution was filtered through a pad of Celite, dried *in vacuo* to afford brown solid which exhibited an IR absorption at 2060 cm^{-1} attributable to coordinated N≡N bonds (Chart S2). Further crystallization of the crude brown solid from THF afforded dark brown block crystals of the dinitrogen- and pyrrolide-bridged Mo(0)–Mo(I) mixed-valence coordination polymer $[(K(N_2)\{Mo(N_2)(\mathbf{PNP})\}_2)_n]\cdot 2thf$ ($\mathbf{2}\cdot 2C_4H_8O$) suitable for a preliminary X-ray analysis (Scheme S2, Fig. S2). **2** is highly reactive, and further purification was not successful.

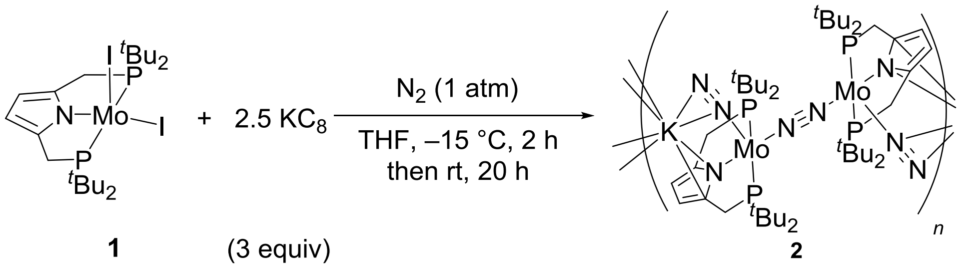

Scheme S2 Preliminary reduction of **1** by KC_8 to afford **2**.

Preparation of $[Li_2L_n\{MoI(N)(PNP)\}_2]$ ($3L_n$) and LiMoI(PNP) (4). To a solution of **1** (73.4 mg, 0.100 mmol) in toluene (5 mL) was added metal lithium shots (7.0 mg, *ca.* 1.0 mmol) at –50 °C under N_2 (1 atm). After the solution was further stirred at –50 °C for 2 h, the mixture was warmed to room temperature, and was further stirred at room temperature for 20 h. The resultant dark purple solution was filtered through a pad of Celite, dried *in vacuo* to afford $[\{Li(PhMe)MoI(N)(\mathbf{PNP})\}_2]$ ($\mathbf{3}(C_7H_8)_2$) as dark brown solid. Further recrystallization of **3** from toluene–*n*-hexane at –20 °C afforded $[\{Li(PhMe)MoI(N)(\mathbf{PNP})\}_2]\cdot 2C_6H_{14}$ ($\mathbf{3}(C_7H_8)_2\cdot 2C_6H_{14}$, 33.7 mg, 0.021 mmol, 42% isolated yield) as brown solid (Scheme S3). IR (KBr, cm^{-1}): 1063 (Mo≡N) (Chart S3). ^1H NMR (C_6D_6, δ): 6.09 (pseudo d, J = 2.3 Hz, C_4H_2N, 4H), 3.04 (pseudo t, J = 4.6 Hz, CH_2, 8H), 1.31 (pseudo t, J = 6.7 Hz, ^{t}Bu, 36H), 1.03 (pseudo t, J = 6.7 Hz, ^{t}Bu, 36H) (Chart S4). $^{31}P\{^1H\}$ NMR (C_6D_6, δ): 95.7 (s) (Chart S5). Anal. Calcd for $C_{70}H_{128}I_2Li_2Mo_2N_4P_4$ ($\mathbf{3}(C_7H_8)_2\cdot 2C_6H_{14}$): C, 52.24; H, 8.02; N, 3.48. Found: C, 52.03; H, 8.42; N, 3.60.

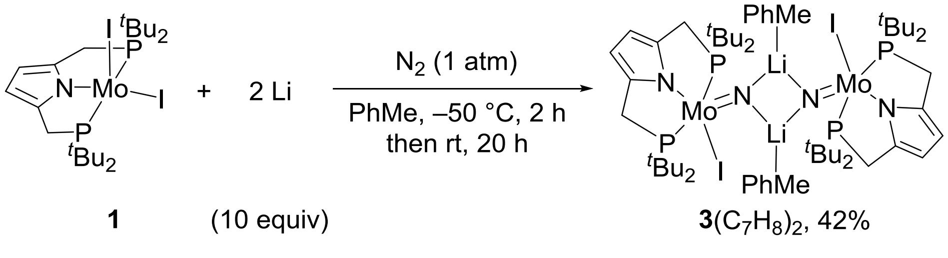

Scheme S3 Preparation of $\mathbf{3}(C_7H_8)_2$ via the cleavage of N_2.

Purple block crystals of $[Li_2(Et_2O)\{MoI(N)(\mathbf{PNP})\}_2]\cdot 0.5Et_2O$ ($\mathbf{3}C_4H_{10}O\cdot 0.5C_4H_{10}O$) (Fig. S3) or purple block crystals of $[\{Li(thf)MoI(N)(\mathbf{PNP})\}_2]$ ($\mathbf{3}(C_4H_8O)_2$) (Fig. S4) suitable for X-ray analyses were obtained by slow evaporation of diethyl ether solution of **3**$(C_7H_8)_2$ at –20 °C or from THF–pentane solution of **3**$(C_7H_8)_2$ at room temperature, respectively, in N_2 glovebox (Scheme S4).

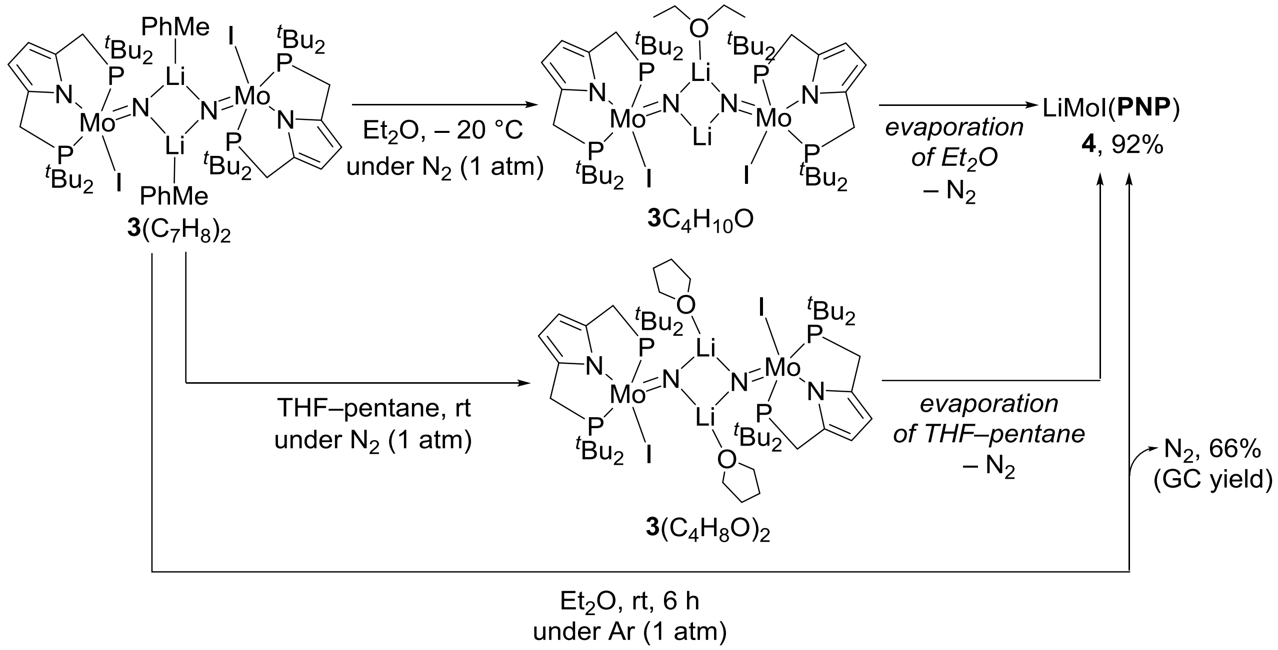

Scheme S4 Preparation of **3**$C_4H_{10}O$, **3**$(C_4H_8O)_2$, and **4** with the evolution of N_2.

Both crystals of **3**$C_4H_{10}O{\cdot}0.5C_4H_{10}O$ and **3**$(C_4H_8O)_2$ are highly efflorescent, thus must be collected for X-ray analyses while crystals are still dipped in solution, otherwise loss of N_2 further occurs to afford LiMoI(**PNP**) (**4**) even in N_2 glovebox. After the slow evaporation of ethereal solution containing crystals of **3**$C_4H_{10}O{\cdot}0.5C_4H_{10}O$, LiMoI(**PNP**) (**4**, 23.5 mg, 0.038 mmol, 92% isolated yield based on **3**$(C_7H_8)_2{\cdot}2C_6H_{14}$ (0.021 mmol) or 38% isolated yield based on **1** (0.100 mmol)) was obtained as a pale orange powder. **4** was also obtained after slow evaporation of THF solution containing **3**$(C_4H_8O)_2$ (Scheme S4). Magnetic susceptibility (Evans' method): $\mu_{\text{eff}} = 1.3$ μ_B in C_4D_8O at 294 K. Anal. Calcd for $C_{22}H_{42}ILiMoNP_2$ (**4**): C, 43.15; H, 6.91; N, 2.29. Found (via slow evaporation of diethyl ether): C, 43.24; H, 6.78; N, 2.22. Found (via evaporation of diethyl ether in vacuo): C, 42.83; H, 7.02; N, 2.33.

The amount of N_2 evolved from **3**$(C_7H_8)_2$ was quantified separately. After a solution of **3**$(C_7H_8)_2{\cdot}2C_6H_{14}$ (32.2 mg, 0.020 mmol) in diethyl ether (5 mL) closed in a 20 mL-Schlenk flask under an atmospheric pressure of argon (1 atm) was stirred at room temperature for 6 h, the aliquot of the gas phase (100 μL) was taken to quantify the amount of dinitrogen by gas chromatography, where the amount of the generated dinitrogen gas (0.013 mmol, 66% yield based on **3**$(C_7H_8)_2$) was calculated based on a calibration curve (Scheme S4).

Catalytic reduction of dinitrogen into ammonia. A typical experimental procedure[S3,S6,S9] for the catalytic reduction of dinitrogen into ammonia using **1** as a catalyst is described below. To a mixture of **1** (1.5 mg, 0.002 mmol) and $SmI_2(thf)_2$ (197.4 mg, 0.360 mmol) placed in a 50 mL-Schlenk flask was added THF (2.5 mL) at room temperature under an atmosphere of dinitrogen (1 atm). Another THF solution (2.5 mL) containing 0.36 mmol H_2O, prepared by mixing 0.13 mL of H_2O (0.72 mmol) with 50 mL of THF in advance, was then introduced to the reaction mixture in one portion at room temperature under an atmosphere of dinitrogen, and the reaction mixture was stirred at room temperature for 18 h in the closed Schlenk flask, where consumption of SmI_2 could be monitored by the color change of the reaction mixture from deep blue to yellow. After the reaction, the aliquot of the gas phase (100 µL) was taken to quantify the amount of dihydrogen by gas chromatography, where the amount of the generated dihydrogen gas (0.136 mmol, 66 equiv/Mo, 75% yield based on $SmI_2(thf)_2$) was calculated based on a calibration curve. Aqueous potassium hydroxide solution (30 wt%, 5 mL) was added to the reaction mixture. The mixture was evaporated under reduced pressure, and the distillate was trapped in a dilute H_2SO_4 solution (0.5 M, 10 mL). The amount of ammonia (0.0230 mmol, 10.2 equiv/Mo, 17% yield based on $SmI_2(thf)_2$) present in the H_2SO_4 solution was determined by the indophenol method.[S10] No hydrazine was detected by the *p*-(dimethylamino)benzaldehyde method.[S11] Detailed results are summarized in Table S1.

Table S1 Catalytic reduction of dinitrogen into ammonia.

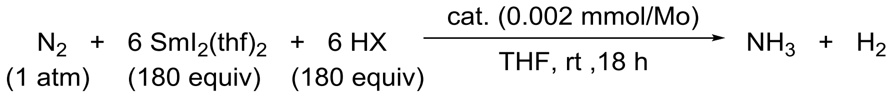

$$\underset{(1\ \text{atm})}{N_2} + \underset{(180\ \text{equiv})}{6\ SmI_2(thf)_2} + \underset{(180\ \text{equiv})}{6\ HX} \xrightarrow[\text{THF, rt ,18 h}]{\text{cat. (0.002 mmol/Mo)}} NH_3 + H_2$$

entry	cat.	reducing reagent	proton source (HX)	NH_3 (equiv)[a]	NH_3 (%)[b]	H_2 (equiv)[a]	H_2 (%)[b]
1	**1**	$SmI_2(thf)_2$	$HOCH_2CH_2OH$	12.2±1.0[c]	20.8±1.7[c]	68±2[c]	77±2[c]
2	**1**	$SmI_2(thf)_2$	H_2O	11.2±0.7[c]	19.1±1.1[c]	67±5[c]	76±6[c]
3[d]	**1**	KC_8[d]	$[H(OEt_2)_2]BAr^F_4$[d]	0.65	5.1[e]	10	53[e]
4[f]	**1**	$CoCp^*_2$[f]	[ColH]OTf[f]	0.34	2.8	15	81
5	**3**$(C_7H_8)_2$	$SmI_2(thf)_2$	$HOCH_2CH_2OH$	6.9	11	71	77
6	**3**$(C_7H_8)_2$	$SmI_2(thf)_2$	H_2O	2.6	4.2	65	71
7	**4**	$SmI_2(thf)_2$	$HOCH_2CH_2OH$	7.3	12	70	77
8	**4**	$SmI_2(thf)_2$	H_2O	2.6	4.2	66	72

[a] Equiv based on the Mo atom of the catalyst. [b] Yield base on the amount of reducing reagent. [c] Average of three runs. [d] 40 equiv of KC_8, 38 equiv of $[H(OEt_2)_2]BAr^F_4$, and 0.01 mmol of **1** as a catalyst in Et_2O at –78 °C for 1 h instead of 180 equiv of $SmI_2(thf)_2$, 180 equiv of HX, and 0.002 mmol of **1** as a catalyst in THF at room temperature for 18 h. [e] Yield base on the amount of proton source ($H(OEt_2)_2]BAr^F_4$) instead of reducing reagent. [f] 36 equiv of $[CoCp^*_2]$, 48 equiv of [ColH]OTf, and 0.01 mmol of **1** as a catalyst in toluene at room temperature for 20 h instead of 180 equiv of $SmI_2(thf)_2$, 180 equiv of HX, and 0.002 mmol of **1** as a catalyst in THF at room temperature for 18 h.

DFT calculations on the conversion between [{Li(thf)MoI(N)(PNP)}$_2$] (3(C_4H_8O)$_2$) and [Li(thf)MoI(N)(PNP)] (A). DFT calculations have been performed for the conversion between [{Li(thf)MoI(N)(**PNP**)}$_2$] (**3**(C_4H_8O)$_2$) and two molar amount of the corresponding monomeric Mo(IV) nitrido complex [Li(thf)MoI(N)(**PNP**)] (**A**).(Scheme S5).

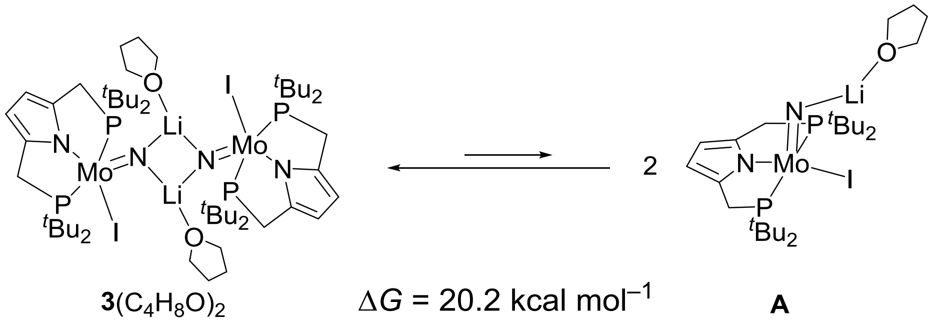

Scheme S5 Conversion between **3**(C_4H_8O)$_2$ and **A**.

DFT calculations were performed with the Gaussian 09 program (Rev. E.01).[S12] Geometry optimizations were carried out with the B3LYP-D3 functional, which is the B3LYP hybrid functional[S13–16] combined with an empirical dispersion correction developed by Grimme.[S17] We employed the SDD (Stuttgart/Dresden pseudopotentials) basis set[S18,S19] for the molybdenum and iodine atoms, and 6-31G(d) basis sets[S20–S23] for the other atoms. Stationary-point structures were confirmed to have the appropriate number of imaginary frequencies by vibrational analysis. To determine the free energy profiles of reaction pathways at 298 K, we performed single-point energy calculations at the optimized geometries using the SDD and 6-311+G(d,p) basis sets.[S24–S26] In the single-point calculations, solvation effects of toluene were taken into account by using the polarizable continuum model (PCM).[S27]

Figure S1 presents optimized structures of **3**(C_4H_8O)$_2$ and **A** and their selected geometric parameters. Cartesian coordinates of the two complexes are listed in Tables S2 and S3. The free energy change (ΔG) for reaction of **3**(C_4H_8O)$_2$ → 2 **A** is calculated to +20.2 kcal/mol in THF at 298 K. This ΔG value implies that the dimeric structure of **3**(C_4H_8O)$_2$ is likely to be maintained in solution at room temperature.

(a)

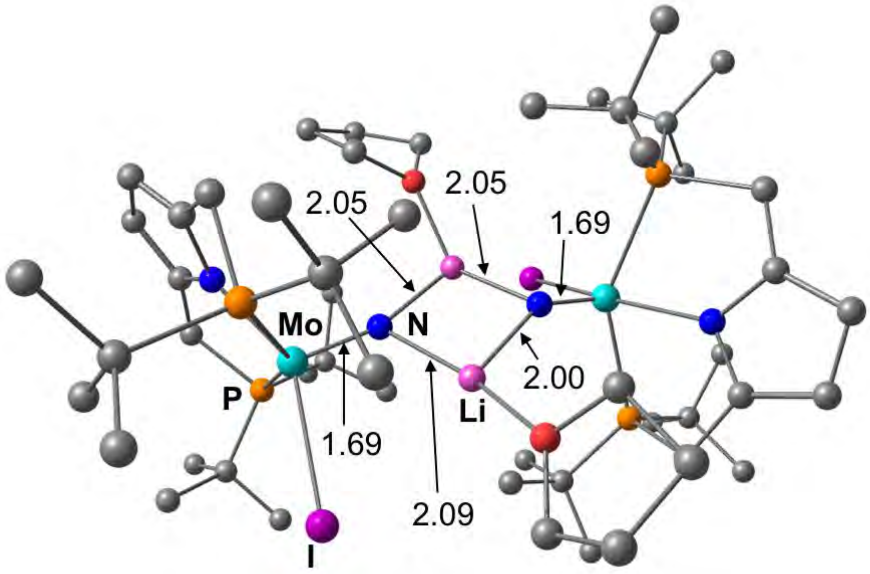

(b)

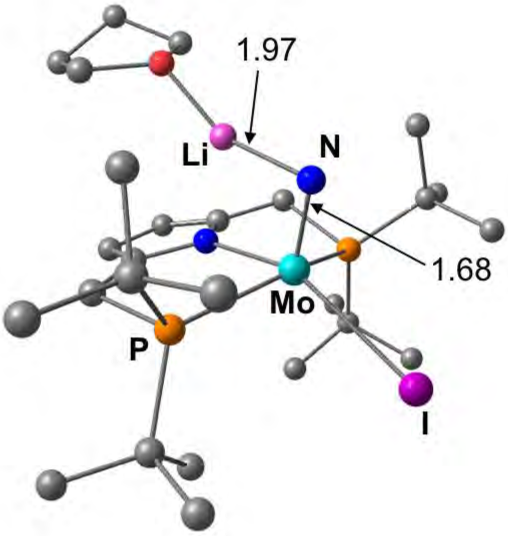

Fig. S1 Optimized structures of (a) [{Li(thf)MoI(N)(**PNP**)}$_2$] (**3**(C_4H_8O)$_2$) and (b) [Li(thf)MoI(N)(**PNP**)] (**A**). Selected interatomic distances are presented in Å. Hydrogen atoms are omitted for clarity.

Table S2 Cartesian coordinate of **3**$(C_4H_8O)_2$ in the closed-shell singlet state. Units are presented in Å.

SCF Energy (opt) = -3951.67970368 hartree

thermal correction (298.15 K) = 1.356454 hartree

SCF Energy (single point in THF) = -3952.51303001 hartree

Atom	Coordinates (Angstroms)		
	X	Y	Z
I	3.073809	2.850552	0.775635
I	-2.554259	-0.988595	-2.841865
Mo	3.041077	0.034535	0.024116
Mo	-3.061109	-0.028216	-0.120232
P	3.750712	0.303385	-2.414011
P	3.629841	-0.822005	2.317714
P	-4.182265	-2.026392	0.945069
P	-3.288171	2.387618	-0.854903
O	0.035895	-3.123278	-0.948222
O	-0.492555	2.113113	2.484969
N	4.169350	-1.742000	-0.348933
N	-4.332849	0.863040	1.330256
N	1.383925	-0.300895	-0.073822
N	-1.505106	-0.099444	0.529413
C	4.944068	-1.127131	-2.651614
H	4.782431	-1.609087	-3.623011
H	5.953343	-0.701891	-2.691904
C	4.843232	-2.094667	-1.510922
C	5.474370	-3.313632	-1.330069
H	6.091592	-3.827505	-2.057496
C	5.194791	-3.734637	0.003816
H	5.526902	-4.648761	0.481516
C	4.402695	-2.756069	0.574912
C	3.804951	-2.649721	1.942405
H	4.397181	-3.189685	2.686421
H	2.792795	-3.068512	1.980334
C	4.799195	1.782830	-3.032714
C	3.900475	3.025642	-3.178321
H	4.529382	3.912145	-3.335515

H	3.299700	3.199093	-2.280442
H	3.232268	2.942456	-4.041831
C	5.563789	1.540041	-4.350917
H	6.215014	0.661429	-4.302606
H	6.207433	2.408254	-4.545949
H	4.904520	1.427033	-5.211682
C	5.844012	2.046287	-1.923007
H	6.487975	2.881394	-2.228754
H	6.495119	1.181165	-1.749206
H	5.373607	2.323080	-0.977546
C	2.329125	-0.103623	-3.630389
C	1.138591	0.831699	-3.363081
H	0.304039	0.555275	-4.017663
H	1.383503	1.880330	-3.549715
H	0.792678	0.748592	-2.331925
C	2.722452	0.000763	-5.115100
H	2.885933	1.036288	-5.425684
H	1.898651	-0.395066	-5.723405
H	3.618245	-0.581911	-5.355912
C	1.893678	-1.556635	-3.347383
H	2.648880	-2.284112	-3.661969
H	0.971084	-1.764641	-3.903834
H	1.689079	-1.726098	-2.290231
C	5.404620	-0.306549	2.859920
C	5.361256	0.949971	3.749856
H	6.386874	1.314781	3.893261
H	4.951404	0.740621	4.742165
H	4.783698	1.756453	3.287100
C	6.187149	0.053789	1.573800
H	7.212998	0.332026	1.851677
H	5.747093	0.919302	1.065530
H	6.241077	-0.782478	0.871849
C	6.167338	-1.434656	3.580278
H	5.638083	-1.814464	4.458216
H	7.135718	-1.045481	3.921194
H	6.372234	-2.272490	2.906639
C	2.404180	-0.788071	3.784565
C	2.043540	0.665612	4.146510

H	1.266100	0.656161	4.922399
H	1.654165	1.208435	3.283823
H	2.890588	1.229002	4.538732
C	1.107426	-1.493217	3.322655
H	0.328673	-1.342741	4.080496
H	1.235356	-2.573523	3.205443
H	0.731429	-1.100341	2.373582
C	2.942431	-1.522251	5.026613
H	3.233262	-2.554172	4.801386
H	2.156229	-1.561411	5.792824
H	3.802126	-1.011523	5.468944
C	-5.550246	-1.220870	1.959422
H	-6.480644	-1.348064	1.392075
H	-5.700605	-1.747205	2.909016
C	-5.255517	0.236031	2.155149
C	-5.863065	1.178563	2.966922
H	-6.640527	0.989027	3.697434
C	-5.305766	2.447595	2.622371
H	-5.553892	3.407481	3.059838
C	-4.379411	2.220594	1.619515
C	-3.494494	3.148950	0.847783
H	-2.487473	3.199377	1.277705
H	-3.895590	4.166269	0.826480
C	-3.117245	-2.904217	2.280574
C	-2.764607	-1.850483	3.350751
H	-2.202720	-1.028973	2.908418
H	-2.131590	-2.323509	4.113757
H	-3.643700	-1.437780	3.854389
C	-1.794549	-3.405892	1.674681
H	-1.941396	-4.116830	0.858861
H	-1.210865	-3.907797	2.458640
H	-1.199277	-2.575479	1.295040
C	-3.842734	-4.082610	2.954371
H	-3.239318	-4.430842	3.802955
H	-3.963493	-4.929622	2.273637
H	-4.828145	-3.806749	3.344240
C	-5.164767	-3.287337	-0.108207
C	-4.174226	-4.232989	-0.812411

H	-3.381135	-3.674193	-1.318875
H	-4.706344	-4.822028	-1.571432
H	-3.717782	-4.939540	-0.110880
C	-6.228055	-4.107803	0.650708
H	-6.798152	-4.702076	-0.075767
H	-6.945259	-3.472057	1.179953
H	-5.796731	-4.804264	1.369857
C	-5.893460	-2.447155	-1.183627
H	-6.493363	-3.116280	-1.814477
H	-5.190618	-1.924706	-1.836132
H	-6.578578	-1.711201	-0.746669
C	-1.869839	3.397677	-1.643802
C	-2.141915	4.911979	-1.594805
H	-1.273467	5.448427	-1.999159
H	-2.303934	5.272422	-0.573419
H	-3.010068	5.189992	-2.200220
C	-0.600311	3.081289	-0.825389
H	0.252656	3.639407	-1.227506
H	-0.352031	2.019252	-0.907589
H	-0.688445	3.349728	0.228955
C	-1.579686	2.963680	-3.095752
H	-1.519143	1.877650	-3.190355
H	-0.610957	3.382774	-3.395675
H	-2.322502	3.328480	-3.805015
C	-4.980337	2.727652	-1.715535
C	-4.813271	2.801430	-3.244259
H	-4.309820	3.719648	-3.558844
H	-5.808319	2.802458	-3.708188
H	-4.261964	1.940992	-3.637928
C	-5.917170	1.535627	-1.407517
H	-5.512722	0.593907	-1.798443
H	-6.878883	1.704447	-1.910864
H	-6.109685	1.422095	-0.338619
C	-5.651764	4.014785	-1.200831
H	-6.576117	4.186831	-1.768308
H	-5.019696	4.899259	-1.325467
H	-5.925694	3.925812	-0.145124
C	1.174176	-3.688609	-0.264097

H	0.810708	-4.248486	0.609601
H	1.788123	-2.853869	0.060170
C	1.870410	-4.605756	-1.287805
H	2.781072	-4.136238	-1.666265
H	2.157572	-5.554964	-0.826411
C	0.809861	-4.794604	-2.407035
H	0.646019	-5.844481	-2.668102
H	1.112470	-4.265067	-3.314600
C	-0.454765	-4.150705	-1.826389
H	-1.108798	-3.674176	-2.556865
H	-1.039475	-4.872440	-1.236074
C	-1.475411	1.554833	3.406357
H	-0.990270	0.745492	3.964072
H	-2.299042	1.153148	2.819658
C	-1.879098	2.705646	4.322614
H	-2.697460	3.273197	3.866540
H	-2.218000	2.351542	5.300661
C	-0.588757	3.535781	4.382207
H	0.128576	3.081781	5.076244
H	-0.748878	4.574758	4.685357
C	-0.075280	3.426441	2.948650
H	-0.537867	4.183109	2.301059
H	1.008092	3.493440	2.844265
Li	-0.324777	-1.238947	-0.700860
Li	0.119365	0.967524	0.999267

Table S3 Cartesian coordinate of **A** in the closed-shell singlet state. Units are presented in Å.

SCF Energy (opt) = -1975.79379717 hartree

thermal correction (298.15 K) = 0.660709 hartree

SCF Energy (single point in THF) = -1976.22292366 hartree

Atom	Coordinates (Angstroms) X	 Y	 Z
Mo	-0.136404	-0.397254	-0.464096
I	-1.068513	-3.127217	-0.747061
P	2.240368	-0.972024	0.241292
P	-2.398859	0.531144	0.138125
O	1.308737	3.779695	-1.303153
N	0.374322	1.291063	0.764494
N	0.089489	0.277871	-1.990040
C	2.732848	0.555576	1.258321
H	3.164681	0.247185	2.212212
H	3.538927	1.081266	0.729695
C	1.545814	1.447745	1.503854
C	1.374048	2.476297	2.414388
H	2.106873	2.820342	3.134796
C	0.047911	2.981306	2.239984
H	-0.418673	3.784160	2.798532
C	-0.538463	2.239061	1.231906
C	-1.905733	2.291321	0.614043
H	-1.902834	2.866403	-0.321387
H	-2.623872	2.784737	1.273947
C	3.494841	-1.011456	-1.210107
C	3.462582	0.347936	-1.942451
H	2.470890	0.547726	-2.358471
H	4.168243	0.311016	-2.782329
H	3.770678	1.184163	-1.304396
C	3.040934	-2.089723	-2.217561
H	3.070022	-3.095687	-1.795151
H	3.714807	-2.073408	-3.085032
H	2.022165	-1.901055	-2.567513
C	4.939129	-1.284819	-0.753192
H	5.613407	-1.202173	-1.615793

H	5.055892	-2.292584	-0.346863
H	5.279793	-0.565321	0.000885
C	2.579970	-2.391529	1.491548
C	2.595660	-3.749498	0.764406
H	1.738042	-3.865856	0.096464
H	2.546812	-4.552626	1.511760
H	3.517835	-3.894735	0.192574
C	3.867924	-2.255169	2.331329
H	3.964836	-3.151788	2.957443
H	3.837956	-1.399403	3.012968
H	4.774306	-2.179259	1.728663
C	1.374090	-2.357568	2.457777
H	1.542998	-3.073916	3.272774
H	0.452611	-2.648668	1.947434
H	1.231120	-1.368648	2.911260
C	-3.735766	0.760204	-1.205914
C	-5.009724	1.446123	-0.683561
H	-5.693848	1.629530	-1.522775
H	-4.792183	2.415042	-0.218528
H	-5.544762	0.828301	0.042997
C	-3.126617	1.625674	-2.333196
H	-3.819278	1.626517	-3.184484
H	-2.167872	1.225954	-2.677431
H	-2.990080	2.671063	-2.033085
C	-4.067937	-0.618557	-1.814303
H	-3.167288	-1.117572	-2.182295
H	-4.758601	-0.477494	-2.656579
H	-4.548550	-1.290660	-1.101925
C	-3.134354	-0.147698	1.778208
C	-4.046453	-1.357910	1.502759
H	-4.986728	-1.066103	1.025559
H	-4.300312	-1.832908	2.459769
H	-3.549702	-2.107722	0.879771
C	-1.934826	-0.631547	2.625223
H	-1.438138	-1.485116	2.155130
H	-2.301373	-0.967523	3.604728
H	-1.198890	0.161124	2.797361
C	-3.902422	0.909664	2.594565

H	-4.371339	0.417714	3.456742
H	-4.695320	1.397747	2.022587
H	-3.233310	1.680565	2.989974
C	2.593314	4.072784	-0.677335
H	3.327238	4.221199	-1.477338
H	2.877038	3.213385	-0.065712
C	2.366369	5.333778	0.155131
H	2.010815	5.052587	1.151539
H	3.276666	5.931111	0.258696
C	1.253687	6.048343	-0.627113
H	1.663476	6.567179	-1.501567
H	0.699943	6.772891	-0.023312
C	0.380021	4.874206	-1.060673
H	-0.302889	4.573648	-0.258208
H	-0.178770	5.045534	-1.984675
Li	0.709844	1.992177	-1.247980

X-ray crystallography. Diffraction data for [MoI$_2$(**PNP**)] (**1**), [(K(N$_2$){Mo(N$_2$)(**PNP**)}$_2$)$_n$]·2thf (**2**·2C$_4$H$_8$O), [Li$_2$(Et$_2$O){MoI(N)(**PNP**)}$_2$]·0.5Et$_2$O (**3**C$_4$H$_{10}$O·0.5C$_4$H$_{10}$O), and [{Li(thf)MoI(N)(**PNP**)}$_2$] (**3**(C$_4$H$_8$O)$_2$) were collected for the 2θ range of 4° to 55° on a Rigaku RAXIS RAPID imaging plate area detector with graphite-monochromated Mo-Kα radiation (λ = 0.71075 Å) with Varimax optics. Intensity data were corrected for empirical (ABSCOR)[S28] absorptions and for Lorentz-polarization effects, while structure solutions and refinements were carried out by using CrystalStructure crystallographic software package.[S29] The positions of the non-hydrogen atoms were determined by direct methods (SHELXS Version 2013/1)[S30] and subsequent Fourier syntheses (SHELXL Version 2016/6),[S31] and were refined on F_o^2 using all unique reflections by full-matrix least-squares with anisotropic thermal parameters except for the following atoms solved isotropically: the oxygen and carbon atoms of solvate diethyl ether molecule (O(3)–C(99)–C(100)) in **3**C$_4$H$_{10}$O·0.5C$_4$H$_{10}$O; one disordered pyrrolide carbon atom (C(26)) and disordered *tert*-butyl carbons (C(42A)–C(43A)–C(44A) and C(42B)–C(43B)–C(44B) solved in a ratio of 0.55:0.45) in **3**(C$_4$H$_8$O)$_2$. All the hydrogen atoms except for nine methyl hydrogen atoms bound to the disordered *tert*-butyl groups ((C(42A)–C(43A)–C(44A) and C(42B)–C(43B)–C(44B)) in **3**(C$_4$H$_8$O)$_2$ were placed at the calculated positions with fixed isotropic parameters. Disorders in **2**·2C$_4$H$_8$O and **3**(C$_4$H$_8$O)$_2$ caused B-level alerts (abnormal U_{eq} difference observed between N(7) and N(8) of the bridging dinitrogen ligand in **2**·2C$_4$H$_8$O; and four isotropic non-hydrogen atoms (C(26), C(42A), C(43A), and C(44A)) with hydrogen atoms missing for the disordered three carbon atoms (C(42A)–C(43A)–C(44A) and C(42B)–C(43B)–C(44C) in **3**(C$_4$H$_8$O)$_2$) in the latest checkCIF/PLATON report. In addition, crystal of **2**·2C$_4$H$_8$O was solved as a merohedral twin. Goodness of fit indicators ($[\Sigma w(F_o^2 - F_c^2)^2/(N_o - N_{param})]^{1/2}$) were all refined to the value of 1.000. Neutral atom scattering factors,[S32] anomalous dispersion effects,[S33] and the values for $\Delta f'$ and $\Delta f''$[S34] as well as for the mass attenuation coefficients[S35] were taken from the literatures. Details of the crystals and data collection parameters are summarized in Table S4. ORTEP drawings and important structural parameters of **1**, **2**·2C$_4$H$_8$O, **3**C$_4$H$_{10}$O·0.5C$_4$H$_{10}$O, and **3**(C$_4$H$_8$O)$_2$ are depicted in Figs. S2–S5 and summarized in Tables S5–S8, respectively. CCDC 1992844 (**1**), 1992845 (**3**C$_4$H$_{10}$O·0.5C$_4$H$_{10}$O), 1995258 (**3**(C$_4$H$_8$O)$_2$), and 2000401 (**2**·2C$_4$H$_8$O) contain supplementary crystallographic data for this paper. These data can be obtained free of charge from The Cambridge Crystallographic Data Centre via www.ccdc.cam.ac.uk/data_request/cif.

Table S4 X-ray crystallographic data for **1**, **2**·$2C_4H_8O$, **3**$C_4H_{10}O\cdot0.5C_4H_{10}O$, and **3**$(C_4H_8O)_2$.

	1	**2**·$2C_4H_8O$	**3**$C_4H_{10}O\cdot0.5C_4H_{10}O$	**3**$(C_4H_8O)_2$
CCDC number	1992844	2000401	1992845	1995258
chemical formula	$C_{22}H_{42}I_2MoNP_2$	$C_{52}H_{100}KMo_2N_8O_2P_4$	$C_{50}H_{99}I_2Li_2Mo_2N_4O_{1.5}P_4$	$C_{52}H_{100}I_2Li_2Mo_2N_4O_2P_4$
formula weight	732.28	1224.29	1363.82	1396.85
crystal size (mm^3)	0.26 × 0.05 × 0.04	0.09 × 0.09 × 0.09	0.52 × 0.10 × 0.10	0.13 × 0.06 × 0.04
color, habit	green, needle	dark brown, block	purple, block	purple, block
crystal system	orthorhombic	orthorhombic	triclinic	monoclinic
space group	*Pbca* (#61)	$P2_12_12_1$ (#19)	$P\bar{1}$ (#2)	$P2_1/n$ (#14)
a (Å)	18.6834(5)	16.2771(4)	15.1684(4)	15.3229(6)
b (Å)	18.4365(6)	18.0042(4)	20.9015(6)	20.6680(9)
c (Å)	16.0574(4)	20.8139(4)	21.1912(5)	20.2145(9)
α (deg)	90	90	84.099(6)	90
β (deg)	90	90	86.660(6)	101.531(7)
γ (deg)	90	90	69.370(5)	90
V (Å^3)	5531.1(3)	6099.6(2)	6252.6(3)	6272.6(5)
Z	8	4	4	4
d_{calcd} (g cm^{-3})	1.759	1.333	1.449	1.479
$F(000)$	2872	2588	2780	2848
μ (cm^{-1})	28.32	6.27	15.27	15.24
transmission factors	0.404–0.893	0.576–0.945	0.691–0.858	0.637–0.941
temperature (°C)	–80	–75	–90	–90
measured reflections	36934	44031	61357	59643
unique reflections	6267	13167	28600	14290
R_{int}	0.0815	0.0945	0.0368	0.1459
refined parameters	266	647	1206	626
$R1$ ($I > 2\sigma(I)$)[a]	0.1137	0.0572	0.0469	0.0746
$wR2$ (all data)[b]	0.2040	0.0635	0.0829	0.1216
GOF[c]	1.000	1.000	1.000	1.000
residual peaks (e Å^{-3})	+2.88/–2.36	+0.86/–0.58	+2.36/–0.88	+2.63/–0.83
Flack parameter		0.000		

[a] $R1 = \Sigma||F_o| - |F_c||/\Sigma|F_o|$. [b] $wR2 = [\Sigma\{w(F_o^2 - F_c^2)^2\}/\Sigma w(F_o^2)^2]^{1/2}$, $w = 1/[\sigma^2(F_o^2) + rP]$, $P = (\mathrm{Max}(F_o^2, 0) + 2F_c^2)/3$ [r = 284 (**1**), –0.1 (**2**·$2C_4H_8O$), 23.15 (**3**$C_4H_{10}O\cdot0.5C_4H_{10}O$), 48.7 (**3**$(C_4H_8O)_2$)]. [c] GOF = $[\Sigma w(F_o^2 - F_c^2)^2/(N_o - N_{param})]^{1/2}$.

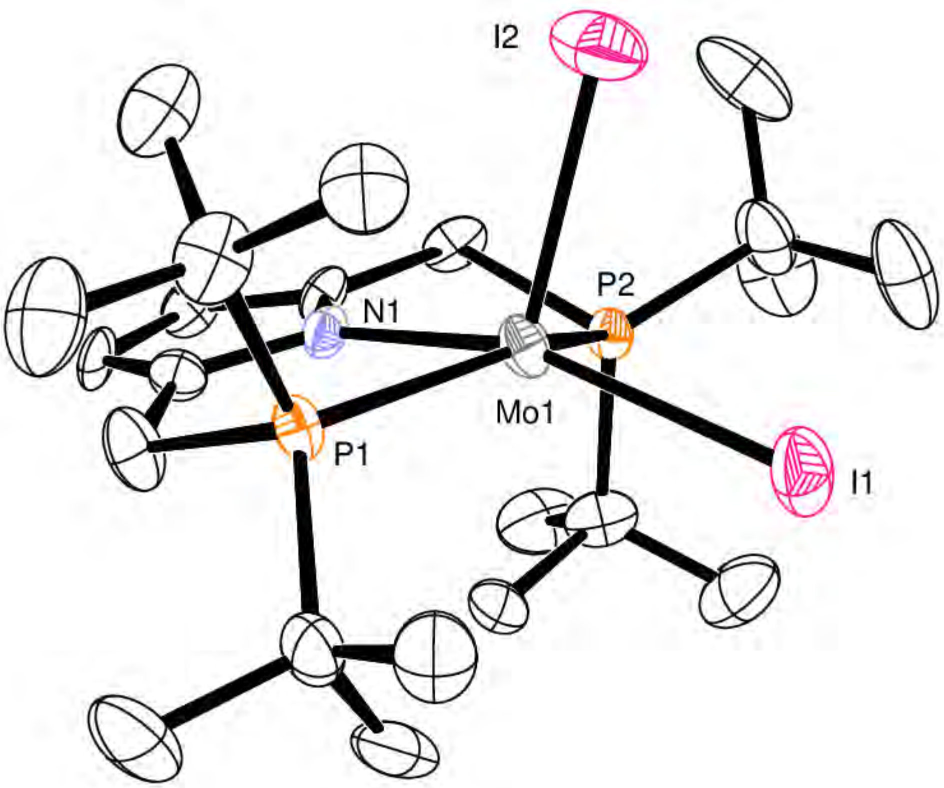

Fig. S2 ORTEP drawing of **1**. Hydrogen atoms are omitted for clarity. Thermal ellipsoids are given at the 50% probability level.

Table S5 Selected bond lengths (Å) and angles (deg) for **1**.

I(1)–Mo(1)	2.7431(14)	I(2)–Mo(1)	2.6464(15)
Mo(1)–P(1)	2.602(3)	Mo(1)–P(2)	2.543(3)
Mo(1)–N(1)	2.084(10)		
I(2)–Mo(1)–I(1)	93.88(5)	P(2)–Mo(1)–P(1)	150.06(11)
P(1)–Mo(1)–I(1)	100.95(8)	P(2)–Mo(1)–I(1)	99.67(8)
P(1)–Mo(1)–I(2)	104.42(8)	P(2)–Mo(1)–I(2)	95.57(8)
N(1)–Mo(1)–I(1)	161.4(3)	N(1)–Mo(1)–I(2)	104.6(3)
N(1)–Mo(1)–P(1)	76.6(3)	N(1)–Mo(1)–P(2)	76.9(3)

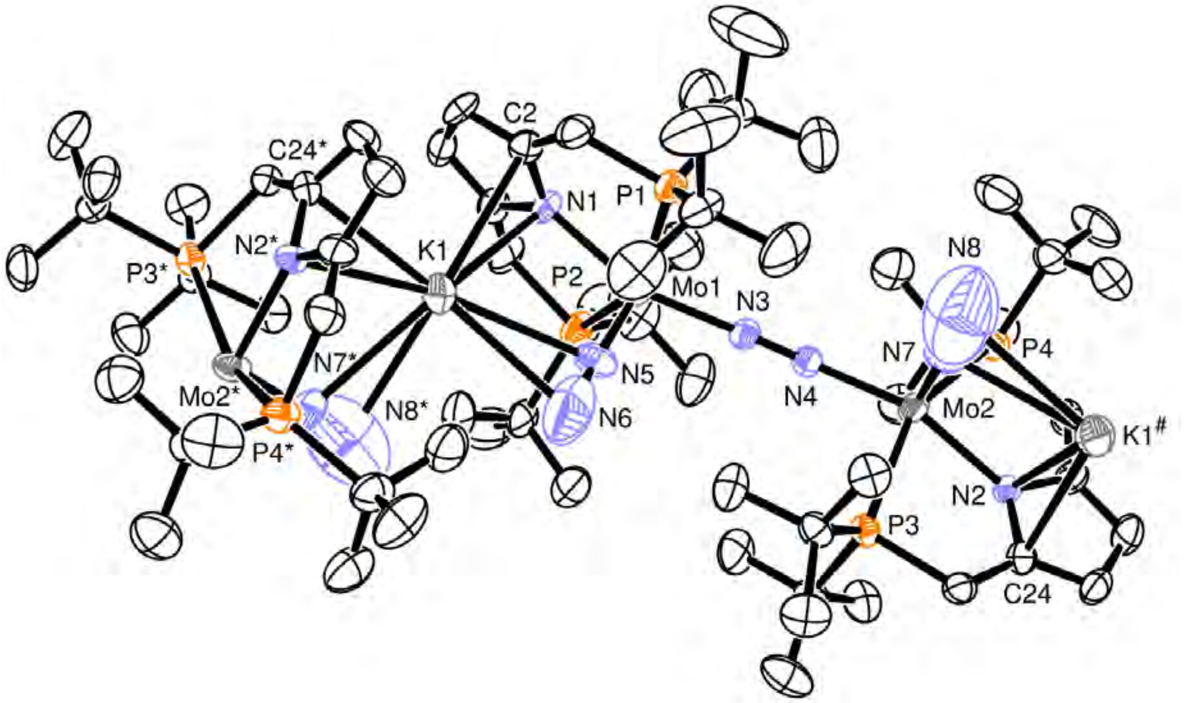

Fig. S3 ORTEP drawing of **2** in an asymmetric unit with its binding proximal moieties (Mo(N_2)(**PNP**) and K) shown. Hydrogen atoms as well as solvate THF molecules are omitted for clarity. Thermal ellipsoids are shown at the 50% probability level.

Table S6 Selected bond lengths (Å) and angles (deg) for $\mathbf{2}\cdot 2\mathrm{C_4H_8O}$.

Mo(1)–N(1)	2.153(5)	Mo(2)–N(2)	2.143(5)
Mo(1)–N(3)	1.991(5)	Mo(2)–N(4)	2.012(5)
Mo(1)–N(5)	1.729(5)	Mo(2)–N(7)	1.686(6)
Mo(1)–P(1)	2.4871(18)	Mo(2)–P(3)	2.4982(17)
Mo(1)–P(2)	2.5103(18)	Mo(2)–P(4)	2.5063(18)
K(1)–N(1)	2.999(5)	K(1)–N(2)*	3.048(5)
K(1)–C(2)	3.042(6)	K(1)–C(24)*	2.965(6)
K(1)–N(5)	2.928(7)	K(1)–N(7)*	2.942(8)
K(1)–N(6)	2.918(8)	K(1)–N(8)*	2.956(14)
N(5)–N(6)	1.116(9)	N(7)–N(8)	1.013(14)
N(3)–N(4)	1.177(5)		

P(2)–Mo(1)–P(1)	151.58(6)	P(4)–Mo(2)–P(3)	150.68(6)
N(1)–Mo(1)–P(1)	76.66(14)	N(2)–Mo(2)–P(3)	76.63(13)
N(1)–Mo(1)–P(2)	77.39(14)	N(2)–Mo(2)–P(4)	77.00(13)
N(3)–Mo(1)–P(1)	96.54(14)	N(4)–Mo(2)–P(3)	95.99(13)
N(3)–Mo(1)–P(2)	103.54(14)	N(4)–Mo(2)–P(4)	102.85(13)
N(5)–Mo(1)–P(1)	99.3(2)	N(7)–Mo(2)–P(3)	100.7(3)
N(5)–Mo(1)–P(2)	97.1(2)	N(7)–Mo(2)–P(4)	97.4(3)
N(3)–Mo(1)–N(1)	158.75(18)	N(4)–Mo(2)–N(2)	155.70(18)
N(5)–Mo(1)–N(1)	101.6(3)	N(7)–Mo(2)–N(2)	102.9(3)
N(5)–Mo(1)–N(3)	99.4(3)	N(7)–Mo(2)–N(4)	101.2(3)
N(5)–K(1)–N(1)	61.24(14)	N(7)*–K(1)–N(2)*	60.25(14)
N(6)–K(1)–N(1)	83.1(2)	N(8)*–K(1)–N(2)*	79.9(3)
N(7)*–K(1)–N(1)	145.66(18)	N(5)–K(1)–N(2)*	152.93(16)
N(8)*–K(1)–N(1)	131.2(3)	N(6)–K(1)–N(2)*	134.3(2)
C(2)–K(1)–N(1)	26.61(14)	C(24)*–K(1)–N(2)*	26.76(13)
C(24)*–K(1)–N(1)	112.43(15)	C(2)–K(1)–N(2)*	114.19(15)
N(2)*–K(1)–N(1)	138.86(13)	C(24)*–K(1)–C(2)	89.43(17)
C(2)–K(1)–N(5)	79.65(16)	C(24)*–K(1)–N(7)*	79.31(17)
C(2)–K(1)–N(6)	101.0(2)	C(24)*–K(1)–N(8)*	98.5(3)
C(2)–K(1)–N(7)*	157.1(2)	C(24)*–K(1)–N(5)	162.32(19)
C(2)–K(1)–N(8)*	154.1(3)	C(24)*–K(1)–N(6)	158.2(2)
N(6)–K(1)–N(5)	22.02(19)	N(8)*–K(1)–N(7)*	19.8(3)
N(7)*–K(1)–N(5)	115.55(16)	N(7)*–K(1)–N(6)	96.5(2)
N(8)*–K(1)–N(5)	97.3(3)	N(8)*–K(1)–N(6)	80.4(3)
C(2)–N(1)–Mo(1)	125.8(4)	C(24)–N(2)–Mo(2)	124.9(4)
K(1)–N(1)–Mo(1)	92.17(16)	K(1)$^{\#}$–N(2)–Mo(2)	90.90(15)
C(2)–N(1)–K(1)	78.4(3)	C(24)–N(2)–K(1)$^{\#}$	73.3(3)
N(4)–N(3)–Mo(1)	174.0(5)	N(3)–N(4)–Mo(2)	167.8(4)
K(1)–N(5)–Mo(1)	104.7(3)	K(1)$^{\#}$–N(7)–Mo(2)	105.2(3)
N(6)–N(5)–Mo(1)	176.2(8)	N(8)–N(7)–Mo(2)	173.9(13)
N(6)–N(5)–K(1)	78.5(6)	N(8)–N(7)–K(1)$^{\#}$	80.9(11)
N(5)–N(6)–K(1)	79.5(6)	N(7)–N(8)–K(1)$^{\#}$	79.3(11)
N(1)–C(2)–K(1)	75.0(3)	N(2)–C(24)–K(1)$^{\#}$	80.0(3)

Symmetry operators: * : ($-x + 1/2$, $-y + 1$, $z + 1/2$), $^{\#}$: ($-x + 1/2$, $-y + 1$, $z + 1/2 - 1$).

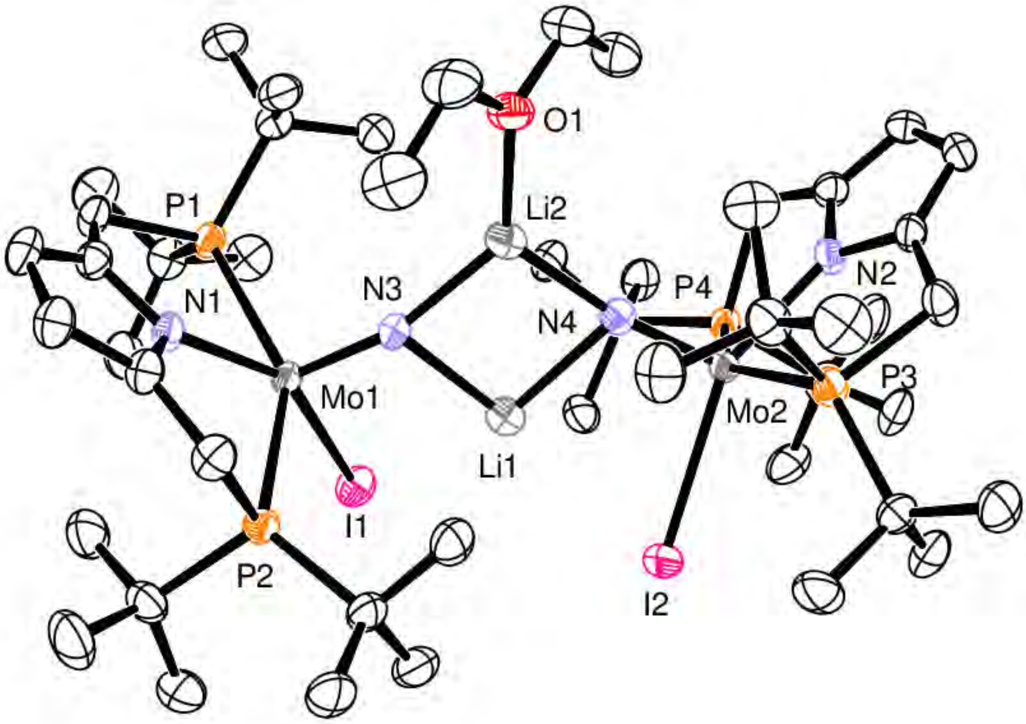

Fig. S4 ORTEP drawing of **3**$C_4H_{10}O$. Only one of the two crystallographically independent structures is shown, with hydrogen atoms and solvate diethyl ether molecule not coordinated to lithium atom omitted for clarity. Thermal ellipsoids are shown at the 50% probability level.

Table S7 Selected bond lengths (Å) and angles (deg) for **3**$C_4H_{10}O\cdot 0.5C_4H_{10}O$.

I(1)–Mo(1)	2.8379(4)	I(2)–Mo(2)	2.8352(5)	I(3)–Mo(3)	2.8387(5)	I(4)–Mo(4)	2.8399(5)
Mo(1)–N(1)	2.106(3)	Mo(2)–N(2)	2.106(3)	Mo(3)–N(5)	2.112(4)	Mo(4)–N(6)	2.101(4)
Mo(1)–N(3)	1.678(3)	Mo(2)–N(4)	1.675(3)	Mo(3)–N(7)	1.679(4)	Mo(4)–N(8)	1.676(4)
Mo(1)–P(1)	2.5506(11)	Mo(2)–P(3)	2.5412(11)	Mo(3)–P(5)	2.5235(11)	Mo(4)–P(7)	2.5403(13)
Mo(1)–P(2)	2.4972(11)	Mo(2)–P(4)	2.4996(10)	Mo(3)–P(6)	2.5318(12)	Mo(4)–P(8)	2.5063(12)
N(3)–Li(1)	2.114(8)	N(4)–Li(1)	2.144(8)	N(7)–Li(3)	2.176(8)	N(8)–Li(3)	2.061(9)
N(3)–Li(2)	1.994(8)	N(4)–Li(2)	1.999(8)	N(7)–Li(4)	2.034(8)	N(8)–Li(4)	2.029(8)
O(1)–Li(2)	1.897(7)			O(2)–Li(4)	1.923(8)		1.923(8)
P(1)–Mo(1)–I(1)	100.85(3)	P(3)–Mo(2)–I(2)	99.40(3)	P(6)–Mo(3)–I(3)	96.04(3)	P(7)–Mo(4)–I(4)	97.48(3)
P(2)–Mo(1)–I(1)	95.44(3)	P(4)–Mo(2)–I(2)	97.15(3)	P(5)–Mo(3)–I(3)	99.71(3)	P(8)–Mo(4)–I(4)	98.12(3)
N(1)–Mo(1)–I(1)	151.26(9)	N(2)–Mo(2)–I(2)	151.63(9)	N(5)–Mo(3)–I(3)	152.12(10)	N(6)–Mo(4)–I(4)	156.34(11)
N(3)–Mo(1)–I(1)	99.47(11)	N(4)–Mo(2)–I(2)	99.41(11)	N(7)–Mo(3)–I(3)	98.07(12)	N(8)–Mo(4)–I(4)	98.04(12)
P(2)–Mo(1)–P(1)	146.51(4)	P(4)–Mo(2)–P(3)	146.46(4)	P(5)–Mo(3)–P(6)	145.67(4)	P(8)–Mo(4)–P(7)	144.60(4)
N(1)–Mo(1)–P(1)	76.28(10)	N(2)–Mo(2)–P(3)	76.36(9)	N(5)–Mo(3)–P(6)	74.89(10)	N(6)–Mo(4)–P(7)	76.40(11)
N(1)–Mo(1)–P(2)	75.42(10)	N(2)–Mo(2)–P(4)	75.24(9)	N(5)–Mo(3)–P(5)	76.99(10)	N(6)–Mo(4)–P(8)	76.60(11)
N(3)–Mo(1)–P(1)	104.67(12)	N(4)–Mo(2)–P(3)	104.40(12)	N(7)–Mo(3)–P(6)	103.89(12)	N(8)–Mo(4)–P(7)	106.54(13)
N(3)–Mo(1)–P(2)	101.20(12)	N(4)–Mo(2)–P(4)	101.38(12)	N(7)–Mo(3)–P(5)	103.83(12)	N(8)–Mo(4)–P(8)	102.47(13)
N(3)–Mo(1)–N(1)	108.97(14)	N(4)–Mo(2)–N(2)	108.85(15)	N(7)–Mo(3)–N(5)	109.65(16)	N(8)–Mo(4)–N(6)	105.61(16)
Mo(1)–N(3)–Li(1)	107.2(3)	Mo(2)–N(4)–Li(1)	107.3(3)	Mo(3)–N(7)–Li(3)	106.6(3)	Mo(4)–N(8)–Li(3)	110.8(3)
Mo(1)–N(3)–Li(2)	164.7(3)	Mo(2)–N(4)–Li(2)	166.8(3)	Mo(3)–N(7)–Li(4)	154.4(3)	Mo(4)–N(8)–Li(4)	155.1(3)
Li(2)–N(3)–Li(1)	85.2(3)	Li(2)–N(4)–Li(1)	84.3(3)	Li(4)–N(7)–Li(3)	83.4(3)	Li(4)–N(8)–Li(3)	86.5(3)
O(1)–Li(2)–N(3)	132.7(4)	O(1)–Li(2)–N(4)	128.0(4)	O(2)–Li(4)–N(7)	134.7(4)	O(2)–Li(4)–N(8)	127.4(4)
N(3)–Li(1)–N(4)	91.2(3)	N(3)–Li(2)–N(4)	99.3(3)	N(8)–Li(3)–N(7)	92.4(3)	N(8)–Li(4)–N(7)	97.7(3)

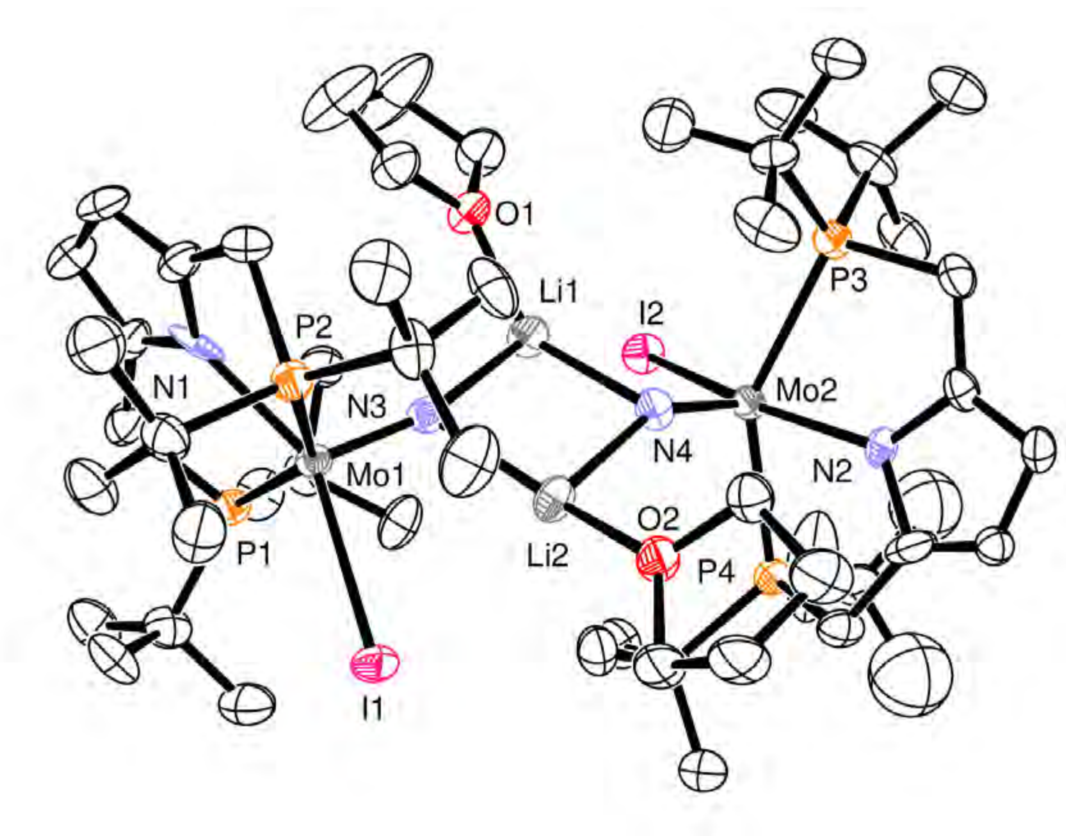

Fig. S5 ORTEP drawing of **3**$(C_4H_8O)_2$. Hydrogen atoms as well as a minor disordered ^{t}Bu group are omitted for clarity. Thermal ellipsoids are shown at the 50% probability level.

Table S8 Selected bond lengths (Å) and angles (deg) for **3**$(C_4H_8O)_2$.

I(1)–Mo(1)	2.8324(8)	I(2)–Mo(2)	2.8445(8)
Mo(1)–N(1)	2.171(7)	Mo(2)–N(2)	2.105(5)
Mo(1)–N(3)	1.681(6)	Mo(2)–N(4)	1.675(6)
Mo(1)–P(1)	2.544(2)	Mo(2)–P(3)	2.530(2)
Mo(1)–P(2)	2.502(2)	Mo(2)–P(4)	2.534(2)
O(1)–Li(1)	1.937(14)	O(2)–Li(2)	2.032(13)
N(3)–Li(1)	2.092(14)	N(4)–Li(2)	2.079(15)
N(3)–Li(2)	2.168(14)	N(4)–Li(1)	2.151(14)
P(1)–Mo(1)–I(1)	98.90(5)	P(3)–Mo(2)–I(2)	101.32(5)
P(2)–Mo(1)–I(1)	96.43(5)	P(4)–Mo(2)–I(2)	94.81(5)
N(1)–Mo(1)–I(1)	150.25(16)	N(2)–Mo(2)–I(2)	153.51(18)
N(3)–Mo(1)–I(1)	99.7(2)	N(4)–Mo(2)–I(2)	99.10(19)
P(2)–Mo(1)–P(1)	146.72(7)	P(4)–Mo(2)–P(3)	146.09(7)
N(1)–Mo(1)–P(1)	76.50(15)	N(2)–Mo(2)–P(3)	76.85(18)
N(1)–Mo(1)–P(2)	75.56(16)	N(2)–Mo(2)–P(4)	75.52(19)
N(3)–Mo(1)–P(1)	104.2(2)	N(4)–Mo(2)–P(3)	103.2(2)
N(3)–Mo(1)–P(2)	102.1(2)	N(4)–Mo(2)–P(4)	103.4(2)
N(3)–Mo(1)–N(1)	109.9(3)	N(4)–Mo(2)–N(2)	107.1(3)
Mo(1)–N(3)–Li(1)	159.7(5)	Mo(2)–N(4)–Li(2)	149.0(5)
Mo(1)–N(3)–Li(2)	111.2(5)	Mo(2)–N(4)–Li(1)	108.8(4)
Li(2)–N(3)–Li(1)	88.5(6)	Li(2)–N(4)–Li(1)	89.3(5)
O(1)–Li(1)–N(3)	105.4(6)	O(2)–Li(2)–N(4)	99.2(6)
O(1)–Li(1)–N(4)	143.8(8)	O(2)–Li(2)–N(3)	158.2(7)
N(4)–Li(1)–N(3)	91.0(5)	N(4)–Li(2)–N(3)	90.9(6)

Table S9 Structural parameters for 5-coordinate Mo nitrido complexes with pincer ligands.

compound[a]	τ[b]	Mo–N length, Å	reference
3$C_4H_{10}O$	0.079	1.678(3)	this work
	0.086	1.675(3)	this work
	0.108	1.679(4)	this work
	0.196	1.676(4)	this work
	0.118±0.047[c]	1.677(4)[c]	this work
3$(C_4H_8O)_2$	0.059	1.681(6)	this work
	0.124	1.675(6)	this work
	0.091±0.032[c]	1.678(7)[c]	this work
[{Na(dmf)Mo(μ_3-N)(NMe_2)(**OCO**)}$_2$]	0.161	1.6601(15)	S37
[Na(15-crown-5)MoI(μ-N)(**POCOP**)]	0.056	1.659(2)	S38
[MoCl(N)(^{t}Bu**PNP**)]	0.108	1.733(9)	S39
[MoCl(N)(^{t}Bu**PNP**)]OTf	0.048	1.634(3)	S39
[MoBr(N)(^{t}Bu**PNP**)]	0.102	1.668(4)	S40
[MoI(N)(^{t}Bu**PNP**)]	0.002	1.685(3)	S40
[MoCl(N)(Ad**PNP**)]BAr^F_4	0.122	1.669(5)	S41
[MoCl(N)(**PNNNP**)]OTf	0.001	1.656(4)	S41
[MoI(N)(Ph-**PNP**)]	0.037	1.672(14)	S42
[MoI(N)(Fc-**PNP**)]	0.031	1.649(11)	S42
[MoCl(N)(H-**PNP**)]BAr^F_4	0.031	1.642(3)	S43
[MoCl(N)(H-**PNP**)]OTf	0.003	1.6463(16)	S43
[MoCl(N)(^{t}Bu**PPP**)]	0.056	1.652(4)	S6
[MoCl(N)(^{t}Bu**PPP**)]BAr^F_4	0.120	1.682(7)	S6
[MoCl(N)(Cy**PPP**)]	0.159	1.656(2)	S44
[Mo(C_2H_4)(N)(Me_2**NNN**)]	0.162[d]	1.653(2)	S45
[Mo(C_2H_4)(N)(H_3Me_2**NNN**)]	0.141[d]	1.6444(16)	S46
[MoCl(N)(**NNN**)]	0.209	1.665(4)[e]	S47
[Mo(N)(OC_6F_5)(**NNN**)]	0.261	1.650(4)	S47
	0.246	1.655(3)	S47
	0.207[e]	1.644(3)	S47
	0.228	1.653(3)	S47
	0.236±0.020[c]	1.651±0.005[c]	S47
[Mo(N)(SAd)(**NNN**)]	0.023	1.6602(12)	S48
[Mo(N)(O^{t}Bu)(H**NNN**)]OTf	0.032	1.6480(13)	S48
[(LutH)Mo(N)(O^{t}Bu)(**NNN**)]BAr^F_4	0.211	1.6811(10)	S48
[Mo(N)(N_3)(**PCCP**)]	0.208[f]	1.6487(6)	S49
[MoI(N)(**PCP**)]I	0.143	1.639(4)	S50
[Mo(N)(O^{t}Bu)(H**ONO**)]	0.258	1.6466(14)	S51
($MePh_3P$)[Mo(N)(O^{t}Bu)(**ONO**)]	0.070	1.6536(16)	S51

[a] Structures of abbreviated pincer ligands are as shown below. [b] Ref S36, calculated based on CIF. [c] Mean value for crystallographically independent units. [d] Calculated based on the mean value for N_{py}–Mo–C_{C2H4}. [e] Based on CIF (different value given in paper). [f] Calculated based on the mean value for N_{az}–Mo–C_{C2H2}.

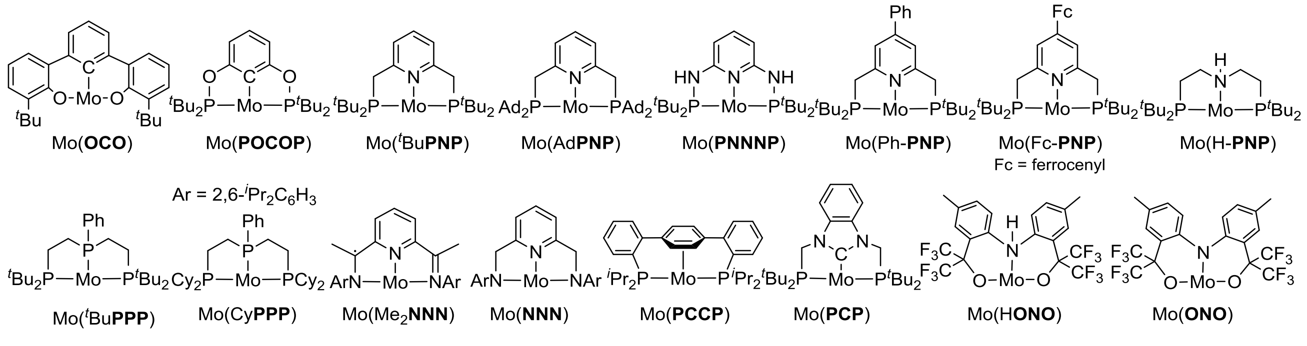

Table S10 Mo–N frequencies for selected 5-coordinate Mo nitrido complexes.

compound	Mo–N vibration, cm^{-1}	reference
[MoX(N)(pincer)]		
3$(C_7H_8)_2$	1063 (KBr)	this work
$[\{Na(dmf)Mo(\mu_3\text{-}N)(NMe_2)(\mathbf{OCO})\}_2]$	1039 (neat)	S37
$[MoCl(N)(^{t}Bu\mathbf{PNP})]$	1031/**1003**^{a} (C_6D_6)	S39
$[MoBr(N)(^{t}Bu\mathbf{PNP})]$	1031 (KBr)	S40
$[MoI(N)(^{t}Bu\mathbf{PNP})]$	1033/**1005**^{a} (KBr)	S40
$[MoCl(N)(^{t}Bu\mathbf{PPP})]$	1031 (KBr)	S6
$[Mo(C_2H_4)(N)(Me_2\mathbf{NNN})]$	1036/**1004**^{a} (KBr)	S45
[Mo(N)(tetradentate tripod)]		
$[Mo(N)(\{3,5\text{-}(2,4,6\text{-}^{i}Pr_3C_6H_2)_2C_6H_3NCH_2CH_2\}_3N)]$	1013 or 1012/**986**^{a} (C_6D_6); 1013 (nujol)	S52; S53
$[Mo(N)(\{3,5\text{-}(2,4,6\text{-}^{t}Bu_3C_6H_2)_2C_6H_3NCH_2CH_2\}_3N)]$	1015/**991**^{a} (C_6D_6)	S53
$[Mo(N)(\{4\text{-}Br\text{-}3,5\text{-}(2,4,6\text{-}^{i}Pr_3C_6H_2)_2C_6H_2NCH_2CH_2\}_3N)]$	1013/**985**^{a} (C_6D_6)	S53
$[Mo(N)\{(3,5\text{-}Me_2C_6H_3NCH_2CH_2)_3N\}]$	1094, 1024 (CsI)	S54
$[Mo(N)\{(3,5\text{-}Me_2C_6H_3NCH_2CH_2)_3N\}]$, polymer-bound	1053, 1028 (CsI)	S54
[Mo(N)(porphyrinato)]		
$[Mo(N)(tpp)](Br_3)$	1014 (nujol)	S55
[Mo(N)(tpp)]	1040 (nujol)	S56
[Mo(N)(tmp)]	1038 (nujol)	S56
[Mo(N)(ttp)]	1047 (nujol)	S56
[Mo(N)(phthalocyaninato)]		
[Mo(N)(pc)]	953 (KBr)	S57
$[Mo(N)(2,3,9,10,16,17,23,24\text{-}^{n}Pr_8\text{-}pc)]$	974 (KBr)	S57
$[Mo(N)(2,3,9,10,16,17,23,24\text{-}^{n}Bu_8\text{-}pc)]$	962 (KBr)	S57
$[Mo(N)\{2,3,9,10,16,17,23,24\text{-}(n\text{-}pentyl)_8\text{-}pc\}]$	974 (KBr)	S57
[Mo(N)(bidentate)$_2$]		
$[Mo(N)(depe)_2]BAr^F_4$	1042/**1010**^{a} (KBr)	S58
[MoX$_2$(N)(bidentate)]		
$[MoCl_2(N)(bpy)]$	948 (nujol)	S59
$[MoBr_2(N)(bpy)]$	949 (nujol)	S55
[MoX$_4$(N)]		
$(Et_4N)[MoCl_4(N)]$	1052 (nujol); 1055 or 1056 (nujol), 1056 or 1055 (Raman, solid)	S60; S61
$(Me_4N)[MoCl_4(N)]$	1054 (nujol); 1058 (nujol), 1050 (Raman, solid)	S62; S61
$(Ph_4As)[MoCl_4(N)]$	1060 (nujol)	S62
$(^{n}Bu_4N)[MoCl_4(N)]$	*1065*, *1032*, *1010* (KBr);^{b} 1063 (nujol), 1065 (Raman, solid)	S63; S61
$(Cl_3PNPCl_3)[MoCl_4(N)]$	995 (nujol)	S64
$[\{Li(12\text{-}crown\text{-}4)\}_2][MoCl_4(N)]_2$	1047 (nujol)	S65
$(MePh_3N)_2[MoCl_4(N)]$	1050 (nujol)	S66
$(Et_4N)_2[MoCl_4(N)]$	1050 (KBr)	S67
$(Ph_4As)[MoF_4(N)]$	969 (nujol)	S68
$(Ph_4P)[MoBr_4(N)]$	1060 (nujol)	S69
$(Ph_4As)[Mo(N)(N_3)_4]$	1040 (nujol)	S70
$(Ph_4P)[Mo(N)(N_3)_4]$	1034 (Raman, solid)	S71
$[Mo(N)(N_3)_2(terpy)][MoN(N_3)_4]\cdot[MoN(N_3)_3(terpy)]$	*1015* (nujol)^c	S72
$(Ph_4P)[Mo(N)(OPh)_4]$	1033 (nujol)	S73
[MoX$_3$Y(N)]		
$[MoCl_3(N)(PPh_3)]$	1109 (nujol)	S74
$[Mo(NPPh_3)_4][MoCl_3(N)(NPPh_3)]_2$	1035, 1028 (nujol)	S75
$[Mo(N)(OSiPh_3)_3(py)]$	1059 (hexane); *1113*, *989* (ATR)^d	S76; S77
$[Mo(N)(OSiMe_3)_3(py)]$	1057 (KBr)	S78
[MoX$_2$Y$_2$(N)]		
$[MoCl_2(N)(PPh_3)_2]$	1049 (nujol); 1049 (nujol), 1045 (Raman, solid)	S69; S71

[Mo(porphyrinato)(μ-N)ML$_n$]		
[Mo(tpp)(μ-N)Mo(CO)$_5$]	*918* (nujol)[c]	S79
[{MoX$_3$(μ-N)}$_4$]		
[{MoCl$_3$(μ-N)}$_4$]	1045 (nujol); 1039 (nujol), 1070, 1023 (Raman, solid)	S80; S74
[{MoBr$_3$(μ-N)}$_4$]	1025 (nujol)	S81
[MoX$_2$(N){(μ-N)ML$_n$}$_2$]		
[Mo(N)(N$_3$)$_2${(μ-N)Mo(N$_3$)(depe)$_2$}$_2$]	*946* (nujol)[c]	S82

[a] ν(Mo≡^{15}N) value shown in **bold**. [b] IR vibration at 1032 cm^{-1} was identified as the ν(Mo≡N) value based on the literatures in ref S63, but 1065 cm^{-1} was cited as the ν(Mo≡N) value in ref. S71. [c] ν(Mo≡N) values mixed and indistinguishable for both five-coordinate and six-coordinate Mo≡N species. [d] Identification of ν(Mo≡N) values not given in the article.

The ν(Mo≡N) value (1063 cm^{-1}) observed for **3**(C$_7$H$_8$)$_2$ is rather blue-shifted compared those reported for the 5-coordinate [MoX(N)(pincer)] species (1031–1039 cm^{-1}).[S6,S37,S39,S40,S45] But the most blue-shifted value has been reported for the μ_3-nitrido ligand coordinated to Na(dmf) ([{Na(dmf)Mo(μ_3-N)(NMe$_2$)(**OCO**)}$_2$]),[S37] suggesting that the Mo≡N vibrations in dimeric structures do not correlate with the activation of Mo≡N bonds. Higher IR vibration has been reported for (^{n}Bu$_4$N)[MoCl$_4$(N)] (1065 cm^{-1})[S63] and [MoCl$_3$(N)(PPh$_3$)] (1109 cm^{-1}).[S74]

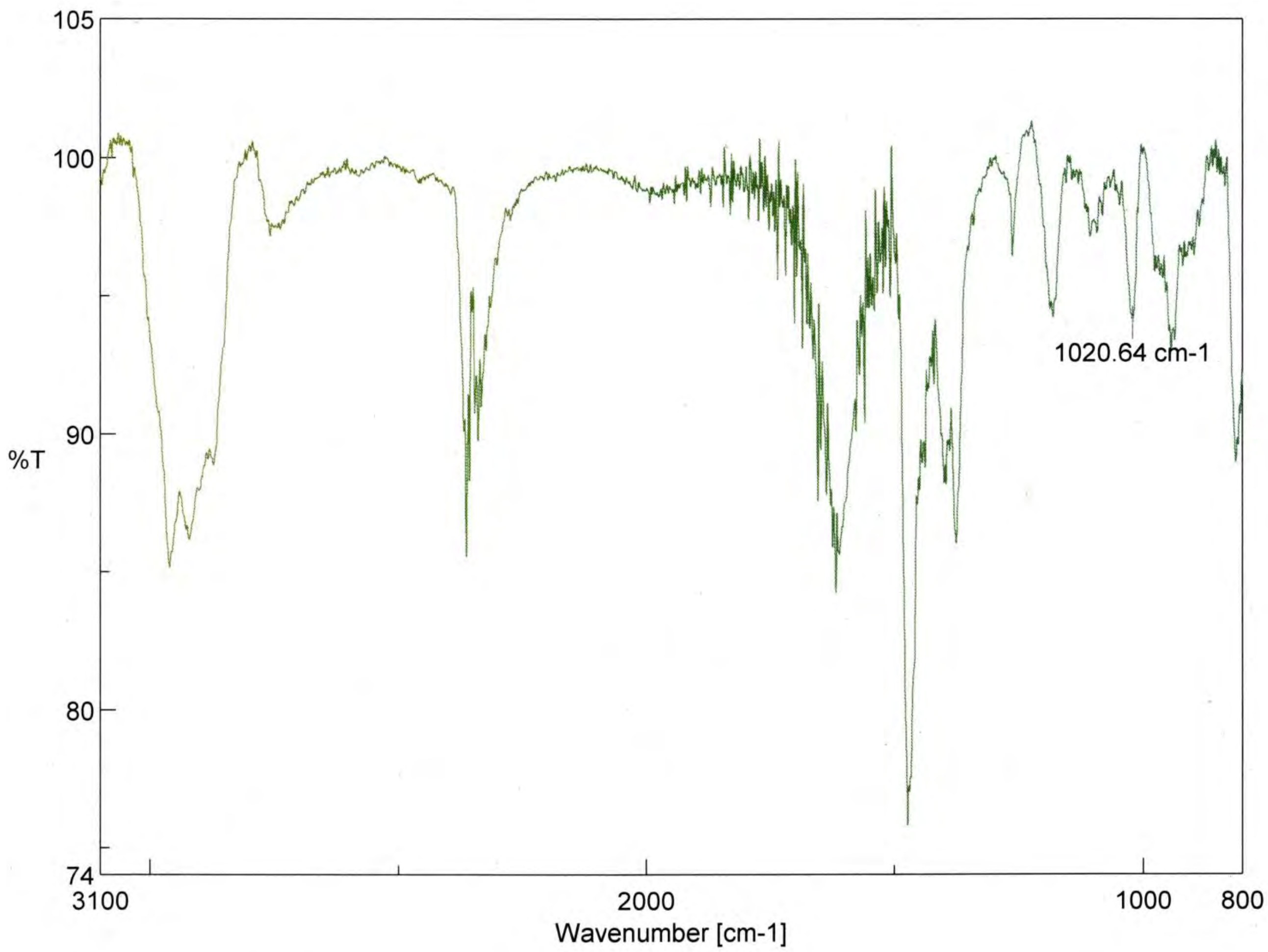

Chart S1 IR spectrum of **1** in a KBr pellet. Absorption value between 1000–1100 cm^{-1} is shown.

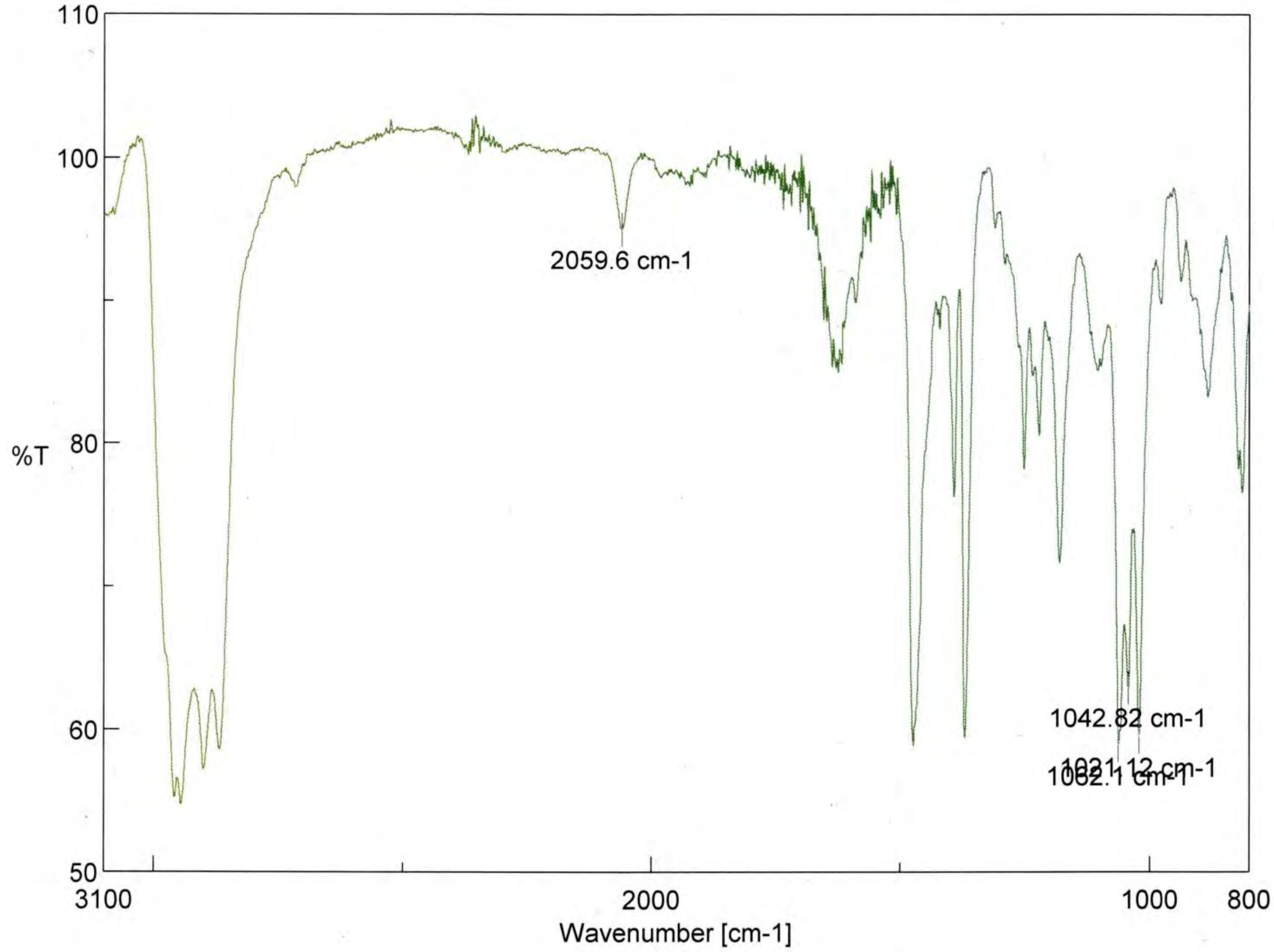

Chart S2 IR spectrum of **2** (crude products) in a KBr pellet. Absorption values between 1000–1100 cm^{-1} as well as those around 1800–2200 cm^{-1} are shown.

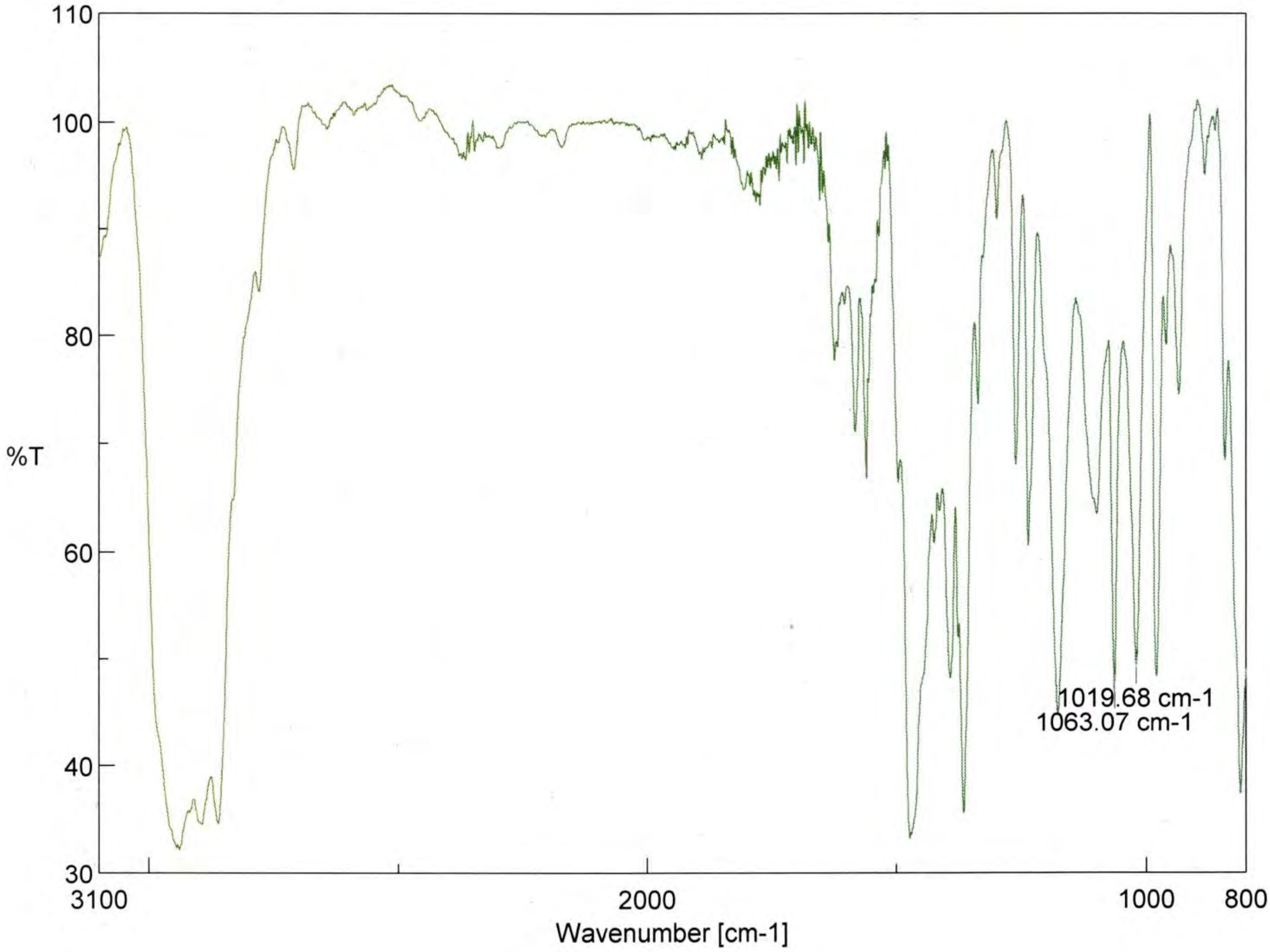

Chart S3 IR spectrum of **3**$(C_7H_8)_2$ in a KBr pellet. Absorption values between 1000–1100 cm^{-1} are shown.

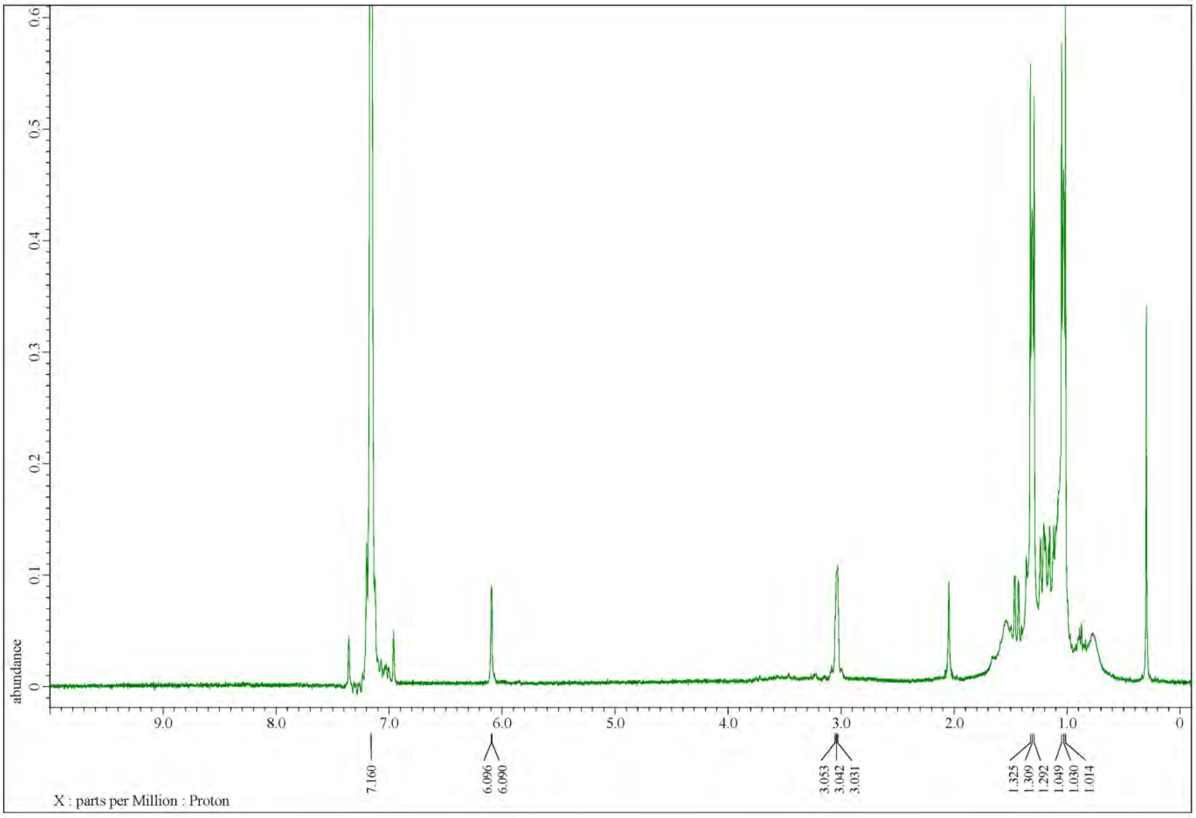

Chart S4 ^{1}H NMR spectrum of **3**$(C_7H_8)_2$ in C_6D_6.

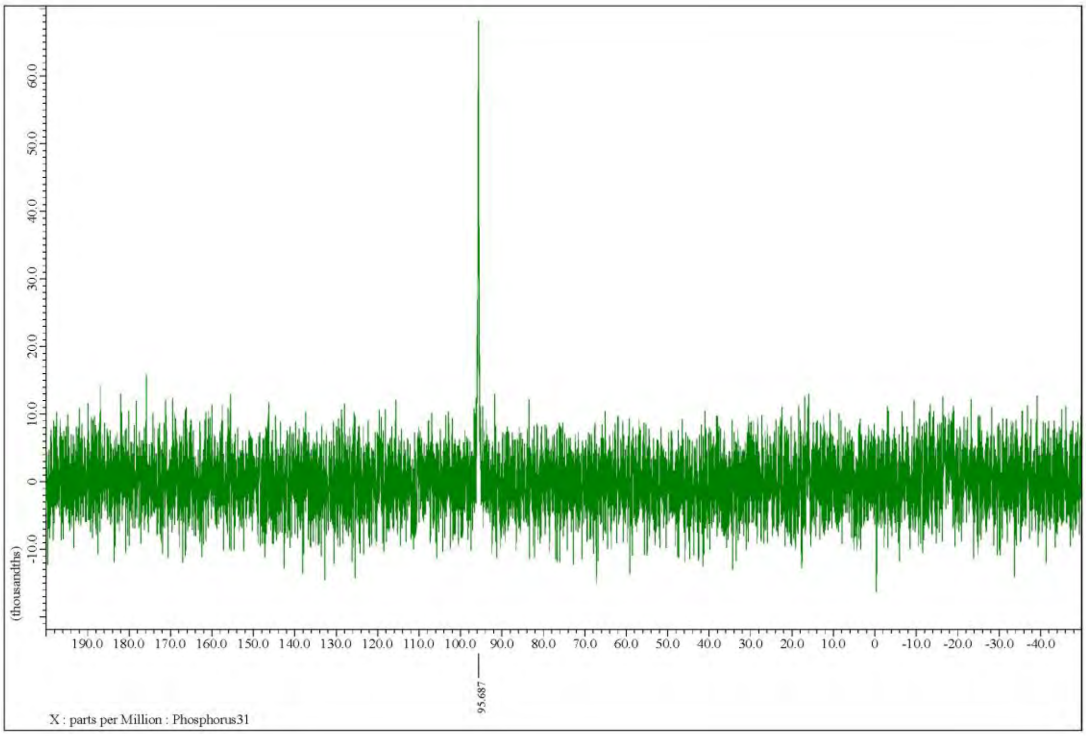

Chart S5 $^{31}P\{^1H\}$ NMR spectrum of **3**$(C_7H_8)_2$ in C_6D_6.

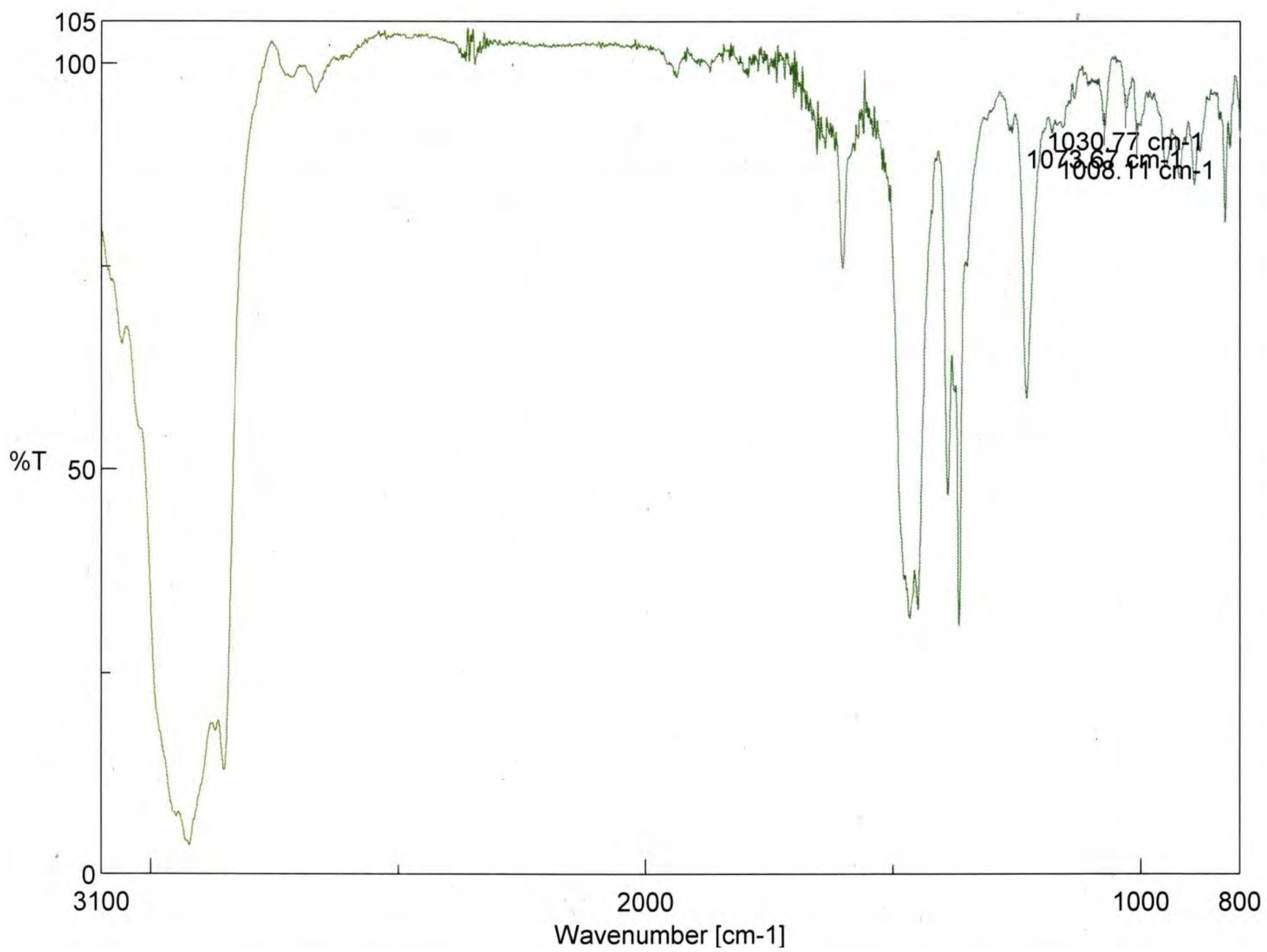

Chart S6 IR spectrum of **4** in a KBr pellet. Absorption values between 1000–1100 cm^{-1} are shown.

References and notes

S1 R. Poli, S. T. Krueger, S. P. Mattamana, K. R. Dunbar and Z. Hanhua, *Inorg. Synth.*, 1998, **32**, 198−203.

S2 S. Kuriyama, K. Arashiba, K. Nakajima, Y. Matsuo, H. Tanaka, K. Ishii, K. Yoshizawa and Y. Nishibayashi, *Nat. Commun.*, 2016, **7**, 12181.

S3 Y. Ashida, S. Kondo, K. Arashiba, T. Kikuchi, K. Nakajima, S. Kakimoto and Y. Nishibayashi, *Synthesis*, 2019, **51**, 3792–3795.

S4 S. V. Yandulov and R. R. Schrock, *Can. J. Chem.*, 2005, **83**, 341–357.

S5 I. S. Weitz and M. Rabinovitz, *J. Chem. Soc., Perkin Trans. 1*, 1993, 117–120.

S6 K. Arashiba, E. Kinoshita, S. Kuriyama, A. Eizawa, K. Nakajima, H. Tanaka, K. Yoshizawa and Y. Nishibayashi, *J. Am. Chem. Soc.*, 2015, **137**, 5666–5669.

S7 M. Brookhart, B. Grant and A. F. Volpe, Jr., *Organometallics*, 1992, **11**, 3920–3922.

S8 G. A. Bain and J. F. Berry, *J. Chem. Educ.*, 2008, **85**, 532–536.

S9 K. Arashiba, A. Eizawa, H. Tanaka, K. Nakajima, K. Yoshizawa and Y. Nishibayashi, *Bull. Chem. Soc. Jpn.*, 2017, **90**, 1111–1118.

S10 M. W. Weatherburn, *Anal. Chem.*, 1967, **39**, 971–974.

S11 G. W. Watt and J. D. Chrisp, *Anal. Chem.*, 1952, **24**, 2006–2008.

S12. M. J. Frisch, G. W. Trucks, H. B. Schlegel, G. E. Scuseria, M. A. Robb, J. R. Cheeseman, G. Scalmani, V. Barone, B. Mennucci, G. A. Petersson, H. Nakatsuji, M. Caricato, X. Li, H. P. Hratchian, A. F. Izmaylov, J. Bloino, G. Zheng, J. L. Sonnenberg, M. Hada, M. Ehara, K. Toyota, R. Fukuda, J. Hasegawa, M. Ishida, T. Nakajima, Y. Honda, O. Kitao, H. Nakai, T. Vreven, J. A. Montgomery, Jr., J. E. Peralta, F. Ogliaro, M. Bearpark, J. J. Heyd, E. Brothers, K. N. Kudin, V. N. Staroverov, T. Keith, R. Kobayashi, J. Normand, K. Raghavachari, A. Rendell, J. C. Burant, S. S. Iyengar, J. Tomasi, M. Cossi, N. Rega, N. J. Millam, M. Klene, J. E. Knox, J. B. Cross, V. Bakken, C. Adamo, J. Jaramillo, R. Gomperts, R. E. Stratmann, O. Yazyev, A. J. Austin, R. Cammi, C. Pomelli, J. W. Ochterski, R. L. Martin, K. Morokuma, V. G. Zakrzewski, G. A. Voth, P. Salvador, J. J. Dannenberg, S. Dapprich, A. D. Daniels, O. Farkas, J. B. Foresman, J. V. Ortiz, J. Cioslowski and D. J. Fox, D. J. Gaussian 09 (Revision E.01), Gaussian, Inc., Wallingford, CT, 2013.

S13. A. D. Becke, *A. Phys. Rev. A*, 1988, **38**, 3098–3100.

S14. A. D. Becke, *J. Chem. Phys.*, 1993, **98**, 5648–5652.

S15. C. Lee, W. Yang and R. G. Parr, *Phys. Rev. B: Condens. Matter Mater. Phys.*, 1988, **37**, 785–789.

S16. S. H. Vosko, L. Wilk and M. Nusair, *Can. J. Phys.*, 1980, **58**, 1200–1211.

S17. S. Grimme, J. Antony, S. Ehrlich and H. Krieg, H., *J. Phys. Chem.*, 2010, **132**, 154104.

S18. M. Dolg, U, Wedig, H. Stoll and H. Preuss, *J. Chem. Phys.*, 1987, **86**, 866–872.

S19. D. Andrae, U. Häußermann, M. Dolg, H. Stoll and H. Preuß, *Theor. Chim. Acta*, 1990, **77**, 123–141.

S20. R. Ditchfield, W. J. Hehre and J. A. Pople, *J. Chem. Phys.*, 1971, **54**, 724–728.

S21. W. J. Hehre, R. Ditchfield and J. A. Pople, *J. Chem. Phys.*, 1972, **56**, 2257–2261.

S22. P. C. Hariharan and J. A. Pople, *Theor. Chem. Acc.*, 1973, **28**, 213–222.

S23. M. M. Francl, W. J. Pietro, W. J. Hehre; J. S. Binkley, M. S. Gordon, D. J. DeFrees and J. A. Pople, *J. Chem. Phys.*, 1982, **77**, 3654–3665.

S24. R. Krishnan, J. S. Binkley, R. Seeger and J. A. Pople, *J. Chem. Phys.*, 1980, **72**, 650–654.

S25. A. D. McLean and G. S. Chandler, *J. Chem. Phys.*, 1980, **72**, 5639–5648.

S26. T. Clark, J. Chandrasekhar, G. W. Spitznagel and P. v. R. Schleyer, *J. Comput. Chem.*, 1983, **4**, 294–301.

S27. J. Tomasi, B. Mennucci and R. Cammi, *Chem. Rev.*, 2005, **105**, 2999–3094.

S28 T. Higashi, ABSCOR: Empirical Absorption Correction based on Fourier Series Approximation, Rigaku Corp., Tokyo, Japan, 1995.

S29 CrystalStructure 4.3: Crystal Structure Analysis Package, Rigaku Corp., Tokyo, Japan, 2000–2019.

S30 G. M. Sheldrick, *Acta Crystallogr., Sect. A: Found. Crystallogr.,* 2008, **A64**, 112–122.

S31 G. M. Sheldrick, *Acta Crystallogr., Sect. C: Struct. Chem.*, 2015, **C71**, 3–8.

S32 E. N. Maslen, A. G. Fox and M. A. O'Keefe in *International Tables for Crystallography, Vol. C*, ed. A. J. C. Wilson, Kluwer Academic Publishers, Dordrecht, 1992, Table 6.1.1.4, pp. 500–503.

S33 J. A. Ibers and W. C. Hamilton, *Acta Crystallogr.*, 1964, **17**, 781–782.

S34 D. C. Creagh and W. J. McAuley in *International Tables for Crystallography, Vol. C*, ed. A. J. C. Wilson, Kluwer Academic Publishers, Dordrecht, 1992, Table 4.2.6.8, pp. 219–222.

S35 D. C. Creagh and J. H. Hubbell in *International Tables for Crystallography, Vol. C*, ed. A. J. C. Wilson, Kluwer Academic Publishers, Dordrecht, 1992, Table 4.2.4.3, pp. 200–206.

S36 A. W. Addison, T. N. Rao, J. Reedijk, J. van Rijn and G. C. Verschoor, *J. Chem. Soc., Dalton Trans.*, 1984, **13**, 1349–1356.

S37 S. Sarkar, A. R. Carlson, M. K. Veige, J. M. Falkowski, K. A. Abboud and A. S. Veige, *J. Am. Chem. Soc.*, 2008, **130**, 1116–1117.

S38 T. J. Hebden, R. R. Schrock, M. K. Takase and P. Müller, *Chem. Commun.*, 2012, **48**, 1851–1853.

S39 H. Tanaka, K. Arashiba, S. Kuriyama, A. Sasada, K. Nakajima, K. Yoshizawa and Y. Nishibayashi, *Nat. Commun.*, 2014, **5**, 3737.

S40 K. Arashiba, A. Eizawa, H. Tanaka, K. Nakajima, K. Yoshizawa and Y. Nishibayashi, *Bull. Chem. Soc. Jpn.*, 2017, **90**, 1111–1118.

S41 E. Kinoshita, K. Arashiba, S. Kuriyama, A. Eizawa, K. Nakajima and Y. Nishibayashi, *Eur. J. Inorg. Chem.*, 2015, 1789–1794.

S42 T. Itabashi, I. Mori, K. Arashiba, A. Eizawa, K. Nakajima and Y. Nishibayashi, *Dalton Trans.*, 2019, **48**, 3182–3186.

S43 G. A. Silantyev, M. Förster, B. Schluschaß, J. Abbenseth, C. Würtele, C. Volkmann, M. C. Holhausen and S. Schneider, *Angew. Chem., Int. Ed.*, 2017, **56**, 5872–5876.

S44 Q. Liao, N. Saffon-Merceron and N. Mézailles, *ACS Catal.*, 2015, **5**, 6902–6960.

S45 G. W. Margulieux, M. J. Bezdek, Z. R. Turner and P. J. Chirik, *J. Am. Chem. Soc.*, 2017, **139**, 6110–6113.

S46 M. J. Bezdek and P. J. Chirik, *Organometallics*, 2019, **38**, 1682–1687.

S47 L. A. Wickramasinghe, T. Ogawa, R. R. Schrock and P. Müller, *J. Am. Chem. Soc.*, 2017, **139**, 9132–9135.

S48 A. K. Hickey, L. A. Wickramasinghe, R. R. Schrock, C. Tsay and P. Müller, *Inorg. Chem.*, 2019, **58**, 3724–3731.

S49 J. A. Buss, C. Cheng and T. Agapie, *Angew. Chem., Int. Ed.*, 2018, **57**, 9670–9674.

S50 A. Eizawa, K. Arashiba, A. Egi, H. Tanaka, K. Nakajima, K. Yoshizawa and Y. Nishibayashi, *Chem. – Asian J.*, 2019, **14**, 2091–2096.

S51 Chakraborty, U. Mandal, I. Ghiviriga, K. A. Abboud and A. S. Veige, *Chem. – Eur. J.*, 2019, **25**, 14059–14063.

S52 D. V. Yandulov, R. R. Schrock, A. L. Rheingold, C. Ceccarelli and W. M. Davis, *Inorg. Chem.*, 2003, **42**, 796–813.

S53 V. Ritleng, D. V. Yandulov, W. W. Weare, R. R. Schrock, A. S. Hock and W. M. Davis, *J. Am. Chem. Soc.*, 2004, **126**, 6150–6153.

S54 A. Wünsche von Leupoldt, C. Förster, T. J. Fiedler, N. H. Bings and K. Heinze, *Eur. J. Inorg. Chem.*, 2013, 6079–6090.

S55 K. Dehnicke, H. Prinz, W. Kafitz and R. Kujanek, *Liebigs Ann. Chem.*, 1981, 20–27.

S56 J. C. Kim, W. S. Rees, Jr. and V. L. Goedken, *Inorg. Chem.*, 1994, **33**, 3191–3194.

S57 K. Frick, S. Verma, J. Sundermeyer and M. Hanack, *Eur. J. Inorg. Chem.*, 2000, 1025–1030.

S58 A. Katayama, T. Ohta, Y. Wasada-Tsutsui, T. Inomata, T. Ozawa, T. Ogura and H. Masuda, *Angew. Chem., Int. Ed.*, 2019, **58**, 11279–11284.

S59 J. Chatt and J. R. Dilworth, *J. Chem. Soc., Chem. Commun.*, 1974, **10**, 517–518.

S60 R. D. Bereman, *Inorg. Chem.*, 1972, **11**, 1149–1150.

S61 N. Ueyama, H. Fukase, H. Zaima, S. Kishida and A. Nakamura, *J. Mol. Catal.*, 1987, **43**, 141–152.

S62 K. Dehnicke and W. Kolitsch, *Z. Naturforsch., B: Anorg. Chem., Org. Chem.*, 1977, **32b**, 1485–1486.

S63 K. Seyferth and R. Taube, *J. Organomet. Chem.*, 1982, **229**, C19–C23.

S64 U. Patt-Siebel, A. Khabou, U. Müller and K. Dehnicke, *Z. Anorg. Alg. Chem.*, 1989, **569**, 91–96.

S65 A. Dietrich, B. Neumüller and K. Dehnicke, *Z. Anog. Allg. Chem.*, 1999, **625**, 619–624.

S66 J. Schmitte, C. Friebel, F. Weller and K. Dehnicke, *Z. Anorg. Allg. Chem.*, 1982, **495**, 148–

156.

S67 C. G. Young, F. Janos, M. A. Bruck, P. A. Wexler and J. A. Enemark, *Aust. J. Chem.*, 1990, **43**, 1347–1355.

S68 D. Fensek, W. Liebelt and K. Dehnicke, *Z. Anorg. Allg. Chem.*, 1980, **467**, 83–88.

S69 K. Dehnicke, N. Krüger, R. Kujanek and F. Weller, *Z. Kristallogr.*, 1980, **153**, 181–187.

S70 K. Dehnicke, J. Schmitte and D. Fenske, *Z. Naturforsch., B: Anorg. Chem., Org. Chem.*, 1980, **35b**, 1070–1074.

S71 R. Haiges, J. A. Boatz, R. Bau, S. Schneider, T. Schroer, M. Yousufuddin and K. O. Christe, *Angew. Chem., Int. Ed.*, 2005, **44**, 1860–1865.

S72 J. Beck and J. Strähle, *Z. Anorg. Allg. Chem.*, 1987, **554**, 50–60.

S73 S. Buth, S. Wocadlo, B. Neumüller, F. Weller and K. Dehnicke, *Z. Naturforsch., B: J. Chem. Sci.*, 1992, **47b**, 706–712.

S74 W. Kolitsch and K. Dehnicke, *Z. Naturforsch., B: Anorg. Chem., Org. Chem., Biochem., Biophys., Biol.*, 1970, **25b**, 1080–1082.

S75 D. Nußhär, F. Weller and K. Dehnicke, *Z. Anorg. Allg. Chem.*, 1993, **619**, 507–512.

S76 H.-T. Chiu, Y.-P. Chen, S.-H. Chuang, J.-S. Jen, G.-H. Lee and S.-M. Peng, *Chem. Commun.*, 1996, **32**, 139–140.

S77 M. Bindl, R. Stade, E. K. Heilmann, A. Picot, R. Goddard and A. Fürstner, *J. Am. Chem. Soc.*, 2009, **131**, 9468–9470.

S78 G.-S. Kim and C. W. DeKock, *Polyhedron*, 2000, **19**, 1363–1371.

S79 J. C. Kim, B. M. Lee and J. I. Shin, *Polyhedron*, 1995, **14**, 2145–2149.

S80 K. Dehnicke and J. Strähle, *Z. Anorg. Allg. Chem.*, 1965, **339**, 171–181.

S81 K. Dehnicke and N. Krüger, *Z. Naturforsch., B: Anorg. Chem., Org. Chem.*, 1978, **33b**, 1242–1244.

S82 D. L. Hughes, M. Y. Mohammed and C. J. Pickett, *J. Chem. Soc., Dalton Trans.*, 1990, **19**, 2013–2019.